Assessing Mesopelagic Zooplankton Food Web Connections at Ocean Station Papa Using Stable Isotope Analysis of Individual Amino Acids

A thesis submitted to the Graduate Division of the University of Hawai‘i at Mānoa in partial fulfillment of the requirements for the degree of

Master of Science

in

Biological Oceanography

December 2021

by

Connor H. Shea

Thesis Committee:
Brian Popp, Chairperson
Erica Goetze
Jeffry Drazen

Acknowledgments

The work presented in this thesis will be published as a collaborative journal article with authorship as follows: Conmnor H. Shea, Paul J. Wojtal, Hilary G. Close, Karen Stamieszkin, Joseph S. Cope, Deborah K. Steinberg, Amy E. Maas, Natalie Wallsgrove, Brian N. Popp. The samples and data described are the products of a large team of scientists working in close collaboration. EXPORTS project planning was lead by David Siegel and Ivona Cetnic. Experimental design for stable isotope analysis was done by Brian N. Popp and Hilary G. Close, and an outreach plan was developed by Brian N. Popp and Kanesa D. Seraphin, who secured funding for this work from the National Science Foundation (NSF Award Numbers: NSF-OCE 1830016, NSF-OCE 1829425). At sea operations were supported by the captain and crew of the *R/V Roger Revelle* and *R/V Sally Ride*. Zooplankton samples were collected and processed by Chandler Countyman, Joseph Cope, Andrea Miccoli, Karen Stamieszkin, and Deborah Steinberg. CSIA-AA of zooplankton samples was done at the University of Hawaii Biogeochemical Stable Isotope Facility by myself and Victor Evrard, with essential support from Tamara Allen and Natalie Wallsgrove. Particles were collected by Claudia Benitez-Nelson, Ken Buesseler, Samantha Clevenger, Steven Pike, Montserrat Roca Marti, Blaire Umhau, and Abigale Wyatt. CSI-AA of particle samples was done by Hilary Close and Paul Kozol Wojtal at the Rosenstiel School of Marine and Atmospheric Science. Sediment trap material was collected by Ken Buesseler, Colleen Durkin, Margaret Estapa, Pat Kelly, Melissa Omand, and Alyson Santoro. Valuable guidance was also given by Moira Decima, Jeff Drazen, Kate Feloy, Erica Goetze, Amy Maas, Liz Miller, David Nicholson, Sonia Romero Romero, Karen Selph, Angel White, and others. Many more scientists than I have listed here contributed to this work indirectly.

Abstract

Constraining how mesopelagic zooplankton communities interact with sinking particle flux is central to building a quantitative understanding of how zooplankton affect the marine carbon cycle. Here, compound specific stable isotope analysis of amino acids is used to quantify food web connections and the contribution of small particles to the base of the mesopelagic zooplankton food web in the Subarctic Northeast Pacific. Samples were collected during the EXPORTS field campaign to Ocean Station Papa in late summer 2018. The δ^{15}N values of source amino acids ($\delta^{15}N_{SAA}$) in zooplankton and small (1-6 μm) particles are similar, which provides strong evidence that the base of the mesopelagic zooplankton food web is composed mainly of 1-6 μm particles. Sinking particulate matter captured in sediment traps, however, have $\delta^{15}N_{SAA}$ values which are lower and similar to what is measured in large (>51 μm) particles. These observations imply that small, suspended particles play an important role in the supply of carbon to the mesopelagic, and that this supply is likely not reflected in sediment trap-derived estimates of carbon flux. The $\delta^{15}N_{SAA}$ values of, and trophic position estimates for chaetognaths suggest that larger predatory taxa in the mesopelagic zone feed on vertically migrating individuals in addition to resident zooplankton at depth. When compared to results from similar studies across the North Pacific, we find that the importance of small particles to the base of the mesopelagic zooplankton food web is highest at sites with low migrant biomass, suggesting a reciprocal relationship between active transport and small particle flux as supplies of carbon to mesopelagic food webs. In addition, comparison of trophic position estimates based on the δ^{15}N values of different combinations of source and trophic amino acids (glutamic acid and phenylalanine vs alanine and phenylalanine) suggests that prostistan heterotrophs are an active component of the zooplankton community down to at least 500 m, and that the length of the zooplankton food web decreases significantly with depth. Our results highlight the importance of small particles and active transport as a source of organic carbon to mesopelagic ecosystems in low productivity areas, emphasizing the need for further work towards distinguishing and quantifying multiple export pathways at mid-water depths.

Contents

1 Introduction **1**

2 Methods **5**
2.1 Sample Collection 5
2.2 Biological metrics 6
2.3 Isotopic analysis 7
2.4 Data Analysis 8

3 Results **11**
3.1 Source amino acid nitrogen isotopic composition of particles 11
3.2 Source amino acid nitrogen isotopic composition of the zooplankton community . . 12
3.3 Source amino acid nitrogen isotopic composition of specific taxa 16
3.4 Source amino acid nitrogen isotope mass balance mixing models 16
3.5 Particle trophic position 19
3.6 Zooplankton trophic position 19
3.7 Zooplankton essential amino acid carbon isotopic fingerprinting 23

4 Discussion **23**
4.1 Assessing the importance of small particles to the mesopelagic zooplankton food web 25
4.2 Assessing the presence of bacterial biomass at the base of the food web 28
4.3 Zooplankton trophic ecology and the role of heterotrophic protists 29
4.4 Implications for active transport as a source of carbon to the mesopelagic 34

5 Conclusion **40**

6 Data Availability **42**

7 Supplemental Data Tables **43**

List of Tables

1 TP parameters 10
2 End member $\delta^{15}\mathrm{N_{SAA}}$ values for the two component $\delta^{15}\mathrm{N_{SAA}}$ mixing model . . . 17
3 Two component $\delta^{15}\mathrm{N_{SAA}}$ mixing model results for size fractionated zooplankton community samples 18
4 Two component $\delta^{15}\mathrm{N_{SAA}}$ mixing model results for taxon specific samples 18
5 $\mathrm{TP_{glu–phe}}$ and $\mathrm{TP_{ala–phe}}$ for specific taxa 22
6 Parameters describing production and particle flux into the mesopelagic 36
7 δ^{15}N values of zooplankton collected in MOCNESS tows. 44
8 δ^{13}C values of zooplankton collected in MOCNESS tows. 45
9 δ^{15}N values of particles collected by in-situ filtration and sediment traps. 46

List of Figures

1 Particle $\delta^{15}\mathrm{N_{SAA}}$ values plotted as a function of depth 13
2 Particles and zooplankton$\delta^{15}\mathrm{N_{SAA}}$ values plotted as a function of depth 15
3 $\mathrm{TP_{glu–phe}}$ and $\mathrm{TP_{ala–phe}}$ for zooplankton and particles plotted against depth . . . 20
4 $\mathrm{TP_{ala–phe}(in-situ)}$ and $\Delta\mathrm{TP_{ala–glu}(in-situ)}$ plotted against depth 21
5 Results from a linear discriminant analysis of mean normalized $\delta^{13}\mathrm{C_{EAA}}$ values of zooplankton community samples 24
6 Fractional contributions of zooplankton size classes to total biomass 26
7 Comparisons of average TP for all zooplankton and 1-6 μm particles plotted against depth 31
8 Predictive Relationships for $\mathrm{f_{small}}$ 35
9 A schematic depicting food web structure throughout the water column at OSP . . 41

Abbreviations

AA: Amino acid
Ala: Alanine
CbPM: Carbon-based production model
CSIA-AA: Compound specific stable isotope analysis of amino acids
EAA: Essential amino acid
EXPORTS: EXport Processes in the Ocean from RemoTe Sensing
GC: Gas chromatograph
Glu: Glutamic acid
Gly: glycine
HNLC: High nutrient low chlorophyll
MOCNESS: Multiple opening closing net and environmental sampling system
IRMS: Isotope ratio mass Spectrometer
LDA: Linear discriminant analysis
Leu: Leucine
Lys: Lysine
MULVFS: Multiple unit large volume filtration system
NASA: North American Space Agency
NPP: Net Primary Productivity
NSF: National Science Foundation
OSP: Ocean Station Papa
PAR: Photosynthetically active radiation
Phe: Phenylalanine
POM: Particulate organic matter
PPZ: Primary production zone
RV: Research vessel
SAA: Source amino acid
TAA: Trophic amino acid
TP: Trophic Position

1 Introduction

Phytoplankton in the euphotic zone use solar energy to fix dissolved inorganic carbon into particulate organic matter, the bulk of which is respired by the euphotic zone community. The remainder (5-25%; Siegel et al. (2014)) sinks and enters the mesopelagic and bathypelagic zones in the form of dead organisms, fecal pellets, and marine snow aggregates. This flux of organic matter is believed to support most heterotrophic life in the deep sea (Robinson et al. 2010), and as these particles sink through the dark water column they are progressively degraded and respired, resulting in the attenuation of carbon flux and increased concentrations of dissolved inorganic carbon at depth (Herndl and Reinthaler 2013). This process, termed the biological pump, is important in regulating air-sea carbon exchange, and its efficiency is generally determined by upper ocean food web processes (Ducklow et al. 2001; Steinberg and Landry 2017).

Although the biological pump is fairly well understood (Ducklow et al. 2001; Herndl and Reinthaler 2013; Steinberg and Landry 2017; Archibald et al. 2019), mesopelagic carbon budgets are often unbalanced with in-situ metabolic activity exceeding organic flux into the mesopelagic (Boyd et al. 1999; Reinthaler et al. 2006; Steinberg et al. 2008). The findings of such studies consistently highlight the need to better characterize and quantify mechanisms of both supply of and demand for carbon to the deep sea (Burd et al. 2010), and while building a better understanding of how the mesopelagic zooplankton community modulates sinking particles could help guide these efforts. However, direct observation of mesopelagic food web interactions is difficult due to the remote nature of the system. Compound specific stable isotope analysis of amino acids (CSIA-AA) provides the ability to probe food web structure without having to observe feeding interactions directly.

CSIA-AA has been used in several recent studies to constrain the relative importance of different size classes of particulate organic matter (POM) to the base of meso- and bathypelagic food webs in the Equatorial and Subtropical North Pacific (Hannides et al. 2013; Gloeckler et al. 2018; Hannides et al. 2020; Romero-Romero et al. 2020). This is made possible by the fact that small, "suspended" particles become highly degraded within the first few hundred meters of the upper water column, resulting in elevated δ^{15}N values in *all* amino acids. This increase in amino acid δ^{15}N values is thought to be caused by extracellular enzymatic hydrolysis of proteins by microbes

(McCarthy et al. 2007; Yamaguchi et al. 2017; Ohkouchi et al. 2017), which occurs to a much greater extent in small, slowly settling or suspended particles (Hannides et al. 2013). On the other hand, larger, faster sinking particles remain relatively unaltered, with amino acid δ^{15}N values similar to what is observed at the surface. Because the δ^{15}N values of source amino acids (SAAs, $\delta^{15}N_{SAA}$) remain relatively unchanged as a result of animal metabolism, increases in $\delta^{15}N_{SAA}$ due to microbial reworking can be traced from particles into higher trophic level zooplankton to understand the particle size distribution at the base of the mesopelagic zooplankton food web. One of the major findings of previous studies is that small, "suspended" particles (< 53 μm) often compose a significant portion of particles at the base of the mesopelagic zooplankton food web (Hannides et al. 2013, 2020; Gloeckler et al. 2018; Romero-Romero et al. 2020). Romero-Romero et al. (2020) found this to be particularly true in systems where particle flux and zooplankton migrator biomass are low. These findings are particularly relevant with regards to carbon budget discrepancies because sediment traps, which are often used to estimate particle flux as a source of carbon to the mesopelagic, are suspected to more efficiently trap large particles (Burd et al. 2010). Therefore, sediment trap material may not be representative of carbon supply at sites where small particles are playing a dominant role at the base of deep sea food webs.

Measurements of the δ^{13}C values of essential amino acids (EAAs, $\delta^{13}C_{EAA}$) can be used to further describe the base of the food web by differentiating phylogenetic groups (e.g., microalgae, bacteria, fungi) responsible for producing the amino acids that are taken up at the base of the food web (Larsen et al. 2009). Recent work has successfully identified specific "patterns" of δ^{13}C values across a suite of essential amino acids (Larsen et al. 2013; Arthur et al. 2014; McMahon et al. 2016; Wall et al. 2021), which reflect different strategies used for carbon acquisition and amino acid biosynthesis among taxonomic groups. These patterns are often highly consistent within taxonomic groups, resulting in a $\delta^{13}C_{EAA}$ "fingerprint" that can be identified using multivariate analyses of $\delta^{13}C_{EAA}$ values (Scott et al. 2006; Larsen et al. 2009). Because most heterotrophic organisms are not capable of de novo synthesis of EAAs, much like SAAs, EAAs are incorporated into metazoan biomass without alteration of their isotopic composition. As a result, $\delta^{13}C_{EAA}$ fingerprints are preserved throughout a food web (Larsen et al. 2009, 2013). While we know that microbes actively degrade particles throughout the water column, and that a significant portion of microbial biomass can be attributed to particle associated bacteria (Mével et al. 2008), the

degree to which microbial biomass becomes incorporated into the mesopelagic zooplankton food web remains unknown. $\delta^{13}C_{EAA}$ fingerprinting is one method that allows us to quantify the contribution of bacterial biomass to the base of the zooplankton food web throughout the water column (Hannides et al. 2013), allowing us to assess the validity of recent hypotheses suggesting microbially mediated trophic upgrading of POM (Mayor et al. 2014).

Trophic structure in the zooplankton community can be elucidated by CSIA-AA to provide an accurate estimate of food web length, largely due to predictable isotopic fractionation that occurs throughout the food web in certain "trophic" amino acids (TAAs; e.g., alanine/ala, leucine/leu, glutamic acid/glu), relative to comparatively non-fractionating SAAs (e.g., glycine/gly, lysine/lys, phenylalanine/phe) (McClelland and Montoya 2002; Popp et al. 2007). As a result, differences between the δ^{15}N values of TAAs and SAAs can be used to calculate trophic position (TP) from a single tissue sample (Chikaraishi et al. 2009; Popp et al. 2007; Bradley et al. 2015). When considered in the context of a mesopelagic carbon budget, calculations of TP can provide estimates of food web length that can affect how we choose to quantify community respiration, and the efficiency with which organic matter is processed by the mesopelagic community.

Recent work, however, has shown that protistan metabolism does not appear to fractionate many of the trophic amino acids that would typically be used to derive estimates of TP (i.e., glutamic acid; Gutiérrez-Rodríguez et al. (2014)). As a result, protistan trophic steps are not accounted for in such estimates. Given that protistan grazers are estimated to remove, on average, 49-67% of daily global primary productivity (Calbet and Landry 2004), it is likely that CSIA-AA based estimates of TP often underestimate trophic position in marine systems (Landry and Décima 2017). Gutiérrez-Rodríguez et al. (2014) and Décima et al. (2017), however, provided strong evidence for unique ^{15}N enrichment in alanine relative to other amino acids during protistan grazing in laboratory chemostat experiments with the dinoflagellate *Oxyrrhis marina*. Following these observations, estimates of TP based on the difference in the δ^{15}N values of alanine and phenylalanine have been applied to derive accurate estimates of trophic position and elucidate food web structure in natural systems with active protistan grazing (Landry and Décima 2017; Décima and Landry 2020; Bode et al. 2021; Landry et al. 2021).

Ocean Station Papa (OSP) in the Subarctic Northeast Pacific is a high nutrient low chlorophyll (HNLC) region, where low rates of primary production are observed throughout the summer

despite replete nutrients, a shallow mixed layer, and sufficient light available for phytoplankton growth (Miller 1993). Instead, iron limitation prevents large cells from effectively competing for the resources required to build their iron-rich photosynthetic reaction centers (Harrison et al. 1999; Strzepek and Harrison 2004), causing the summertime algal community to be dominated by small, prokaryotic algae. Meanwhile, protistan microzooplankton graze heavily upon the prokaryotic community at a rate closely matching primary production, resulting in a low standing stock of algal biomass throughout the summer (Landry et al. 1993; McNair et al. 2021). Protistan microzooplankton, in turn, act as a trophic link connecting the microalgal community to the mesozooplankton food web. Thus, the euphotic zone at OSP represents a relatively long food web organized around efficient utilization of organic matter produced by an iron-limited microalgal community. Finally, Goldblatt et al. (1999) describes a shift from an algae-based food web in the mixed layer to a detritus-based food web below. Beyond this, little information exists about how the mesopelagic zooplankton community is structured at OSP or on the resources that form its base, both of which have consequences for the efficiency with which carbon is exported in this and other similar systems.

Here we use CSIA-AA to constrain mesopelagic zooplankton food web connections in the Subarctic Northeast Pacific, extending our knowledge of food web structure below the euphotic zone. The work was carried out within the context of the NASA EXPORTS mission to Ocean Station Papa (Siegel et al. 2021) and leveraged against ancillary data sets to help address one of the key science questions identified in the EXPORTS science plan (Siegel et al. 2015): *"what controls the efficiency of vertical transfer of organic matter below the well-lit surface ocean?"* To address this question, we compared $\delta^{15}N_{SAA}$ values in particles, size fractionated zooplankton, and specific zooplankton taxa to assess the contribution of small particles to the base of the mesopelagic zooplankton food web, as well the role of vertically migrating zooplankton as conduits of fresh material from the surface. These results are compared to similar studies conducted elsewhere in the North Pacific in order to draw conclusions about ocean basin scale trends in mesopelagic food web dynamics. The $\delta^{15}N$ values of source and trophic amino acids are also used to estimate trophic position and food web length, specifically quantifying contributions of mesopelagic protozoa grazing to the food web. Finally $\delta^{13}C_{EAA}$ fingerprinting is used to assess the relative importance of microbial biomass to the base of the food web.

2 Methods

2.1 Sample Collection

Samples were collected from Ocean Station Papa (location: 50.1°N, 144.9°W) as part of the multi-ship, NASA-lead EXPORTS field campaign (August 15 to September 7, 2018; Siegel et al. (2021)). Cruise activities were divided into three, 8-day sampling cycles, or epochs, with each epoch tracking a water parcel in a Lagrangian manner.

Zooplankton were collected from the *RV Roger Revelle* using a 1 m^2 MOCNESS (Multiple Opening/Closing Net and Environmental Sensing System; Wiebe et al. (1985)) using ten 200 μm nets and equipped with sensors to measure conductivity, dissolved oxygen, temperature, pressure, fluorometry, flow through the net, and net angle. The nets were deployed during six sets of paired day-night tows, two sets in each epoch, and targeted depths of 0-50, 50-100, 100-150, 150-200, 200-300, 300-400, 400-500, 500-750, and 750-1000 m. The contents of the cod end were split and one quarter was separated by size fraction using nested sieves of 5.0, 2.0, 1.0, 0.5, and 0.2 mm mesh, and then rinsed with filtered seawater followed by isotonic ammonium formate over pre-weighed 0.2 mm mesh nitex filters before being frozen at -20°C for biomass and stable isotope analysis. CSIA-AA was done on zooplankton from tows 88 and 89 in epoch 2. The 0.2-0.5 and 1-2 mm size classes were analyzed in all depth strata, day and night. The 2-5 and >5 mm size fractions were only analyzed in the 0-50, 50-100, 300-400, and 500-750 m depth strata from the nighttime tow. Nighttime tows were analyzed in particular to capture the zooplankton community when vertically migrating individuals were at their most likely depth of feeding and the specific depths were chosen to provide adequate water column coverage without analyzing samples from all depths. Radiolarians were removed from all frozen samples prior to analysis and analyzed separately.

Another quarter of the cod end material was preserved in sodium borate buffered 4% formaldehyde solution for taxonomic analysis. Salps were removed from all samples and results from CSIA-AA of their tissue is presented in Doherty et al. (2021). CSIA-AA of specific taxa were performed on animals separated from formalin preserved samples, and rinsed thoroughly prior to analysis. 1-2 mm *Neocalanus spp.* were numerically abundant throughout the water column during the cruise and were isolated (100 individuals) from the 500-750 m, nighttime depth strata

in order to capture this taxa during its ontogenetic migration to depth. 1-2 mm *Metridia spp.* (40 individuals) were taken from the 0-50 m, nighttime depth strata to characterize the isotopic composition of a known vertical migrator. Chaetognaths were a numerically abundant component of the mesopelagic community and were isolated (15-20 individuals) from the 2-5 and >5 mm size fractions in the 300-400 and 500-750 m depth strata in nighttime tows. As known carnivores, chaetognaths were examined for their predatory role in the food web. Radiolarians are protists and opportunistic predators and individuals of the >5 mm size fraction were isolated from daytime and nighttime tows at 500-750 m. These depths were chosen for chaetognaths and radiolarians so that they could be compared to whole zooplankton community samples of the 2-5 and $>$ 5 mm size fractions.

Particulate material was obtained using in-situ filtration (Large Volume Water Transfer System, McLane Labs). Each pump was fitted with two separate 142-mm diameter mini-MULVFS (Multiple Unit Large Volume Filtration System) filter holders as in Lam et al. (2015). Pumps were deployed from the *RV Sally Ride* to 50, 95/105, 145/155, 195/205, 330, and 500 m and water was filtered through a series of 51 and 5 or 6 μm Nitex mesh (nylon), 1 μm QMA (quartz microfiber), and sometimes 0.3 μm GF75 (glass fiber) filters. Pump depths were verified by a pressure sensor on the deepest pump. CSIA-AA was done on particles from all epochs. Surface tethered and neutrally buoyant sediment traps were deployed for 3-6 days at discrete depths between the base of the euphotic zone (0.1% PAR) and 510 m. Sediment trap deployments are described in detail in Estapa et al. (2020).

2.2 Biological metrics

Zooplankton biomass and migrator biomass were determined as in Steinberg et al. (2008). After collection, the frozen splits of zooplankton were measured for wet and dry weight. Formalin preserved samples were diluted and subsampled with a 10-ml Stempel pipette, such that an approximate minimum of 100 animals was counted and identified (mean=232 animals per sample). In samples with low animals counts, the whole sample was analyzed. Taxonomic identification and enumeration were done under a Leica dissecting microscope (MZ16).

2.3 Isotopic analysis

Zooplankton samples were processed at the University of Hawaii in the Biogeochemical Stable Isotope Facility, and particles at the University of Miami Marine Organic Isotope Geochemistry Lab, all using routine procedures outlined in Hannides et al. (2009). Briefly, amino acids were isolated and purified by hydrolysis in 6N hydrochloric acid followed by cation exchange chromatography. The purified amino acids were then treated with isopropanol and trifluoroacetic acid yielding trifluoroacetic amino acid esters. The resulting solution was further purified by liquid-liquid extraction into chloroform before being stored in a dichloromethane-trifluoroacetic acid solution, and then finally transferred into ethyl acetate just prior to mass spectrometric isotopic analysis. CSIA-AA was carried out on a gas chromatograph coupled to an isotope ratio mass spectrometer (GC-IRMS), with all samples measured in triplicate when amino acid concentrations were sufficient.

The nitrogen isotopic composition of zooplankton was measured using a Thermo Scientific Delta V Plus IRMS interfaced to a Trace gas chromatograph fitted with a 60 m BPx5 capillary column (SGE Analytical Science, 0.32 mm diameter, 1 μm stationary phase) via a GC-C III combustion interface (980 °C) with reduction furnace (650 °C)) and liquid nitrogen cold trap. Internal reference compounds, L-2-Aminoadipic acid (AAA) and L-(+)-Norleucine (NOR) of known nitrogen isotopic composition, were co-injected with samples and used to determine accuracy and precision. The nitrogen isotopic composition of particle samples was measured on a Thermo Fischer Scientific MAT 253 Plus IRMS interfaced to a Trace 1310 GC fitted with a 50 m BPx5 capillary column (Trajan, 0.32 mm diameter, 1.0 μm stationary phase) via a GC Isolink II system with a combined oxidation/reduction reactor (1000 °C), liquid nitrogen cold trap, and Conflo IV interface. During analysis of both zooplankton and particles, a suite of 14 pure amino acids of known isotopic composition were co-injected with noroleucine and aminoadipic acid and measured every 2-4 sample injections as a reference material. The results from analyses of the amino acids suite were used to derive a linear correction to normalize measured sample amino acids δ^{15}N values to AIR. Corrected results are reported in δ-notation relative to atmospheric N_2.

The carbon isotopic composition of zooplankton was measured using a Thermo Scientific MAT 253 IRMS interfaced to a Trace GC Ultra gas chromatograph fitted with a 30 m BPx5 capillary

column (SGE Analytical Science, 0.32 mm diameter, 1 μm stationary phase) and PTV injector, via a GC Isolink combustion interface (1000 °C) and a Thermo Scientific Conflo IV continuous flow interface. A suite of 14 pure amino acids of known isotopic composition were co-injected with NOR and AAA as well as $\mathrm{n-C_{20}}$ alkane of known carbon isotopic composition, measured immediately before and after triplicate injections, and used for isotopic correction calculations to normalize measured sample amino acid δ^{13}C values to V-PDB. All sample δ^{13}C values were corrected for the addition of carbon during derivitization using the methods of Silfer et al. (1991). Isotope results are reported in δ-notation relative to V-PDB. Standard deviations are derived from the variance of at least three injections, but when less than three injections were possible instrument precision was used as an estimate of uncertainty.

Instrument accuracy was determined by co-injecting noroleucine and aminoadipic acid with each sample and calculating the difference between their known isotopic composition and that which was measured during analysis. Whichever compound gave a greater difference between known and measured δ^{15}N values was used as a conservative estimate of accuracy for that run. When averaged across all analyses, both, we estimate an instrument accuracy of $\pm 1.0‰$ for this study. Instrument precision was determined by calculating the standard deviation of the isotopic compositions measured for noroleucine and aminoadipic acid over the course of a day. Whichever gave a larger standard deviation was used as a conservative estimate analytical precision for the instrument on that day. When averaged across all analyses, both carbon and nitrogen, we estimate an instrument precision of $\pm 0.3‰$. The average standard deviation of sample δ^{15}N and δ^{13}C values was 0.4 ‰.

2.4 Data Analysis

The fractional contribution of small (1-6 μm) and large (6-51 and >51μm) particles to the base of the mesopelagic zooplankton food web was assessed using a two-component isotope mass balance mixing model (Phillips and Gregg 2001) based on $\delta^{15}\mathrm{N_{SAA}}$ values, as in Hannides et al. (2013). Glycine, serine, phenylalanine, and lysine were used as representative source AA's, and their δ^{15}N values were averaged to calculate $\delta^{15}\mathrm{N_{SAA}}$. Mixing models were evaluated for each zooplankton collection depth strata. Particle end member $\delta^{15}\mathrm{N_{SAA}}$ values were determined by

averaging the $\delta^{15}N_{SAA}$ values of samples within the depth strata that zooplankton were collected. When no data from particles were available with a zooplankton depth strata, $\delta^{15}N_{SAA}$ values were inferred by linear interpolation using samples from adjacent depths. The maximum depth was set at 500 m, which was the deepest depth of particle collection. Uncertainty in the fractional contribution of small (1-6 μm) and large (>51 μm) particles to the base of the food web (f_{small} and f_{large}, respectively) were estimated by propagating error in $\delta^{15}N_{SAA}$ values as described in Phillips and Gregg (2001). To aggregate mixing model results, means and biomass weighted averages were calculated. Weighting factors for the biomass weighted averages were calculated from dry weights of zooplankton in depth stratified and size fractionated MOCNESS samples. Weighting factors were applied within a depth, size class, or both, depending on how the data were being aggregated and interpreted. Uncertainty in f_{small} was propagated through averages using standard rules of error propagation (Taylor 1997).

Trophic position was calculated from $\delta^{15}N$ values of amino acids using the equation:

$$TP = \frac{\delta^{15}N_{tr} - \delta^{15}N_{src} + \beta_{tr-src}}{TDF_{tr-src}} + 1 \quad (1)$$

where $\delta^{15}N_{tr}$ and $\delta^{15}N_{src}$ are the $\delta^{15}N$ values associated with some specified individual or set of trophic and source amino acids, β is the difference between $\delta^{15}N_{tr}$ and $\delta^{15}N_{src}$ in primary producers, and TDF (the trophic discrimination factor) describes how much $\delta^{15}N_{tr}$ changes relative to $\delta^{15}N_{src}$ with each trophic step. Both β and TDF are determined empirically, and specific to the set of amino acids used. TP was estimated using three different sets of amino acids, which are tabulated along with their respective β values and TDFs in Table 1. $TP_{ala-phe}$ was used to estimate total food web length, inclusive of protistan heterotrophy, as in Décima and Landry (2020). Because error was not reported in Décima and Landry (2020), estimates of error in $TDF_{ala-phe}$ and $\beta_{ala-phe}$ from Décima et al. (2017) were used and are considered conservative. $TP_{glu-phe}$ was used to estimate the length of the metazoan food web, exclusive of protistan heterotrophy, as in Chikaraishi et al. (2009). These two estimates of TP were then compared by subtracting $TP_{glu-phe}$ from $TP_{ala-phe}$ to obtain $\Delta TP_{ala-glu}$, in order to estimate the number of protistan trophic steps present in the food web, and error was propagated through that calculation. TP_{tr-src} is also reported here and was calculated using glutamic acid, alanine, and leucine as

Table 1: The source and trophic amino acids, β values, and TDFs, associated with each formulation of TP used in this study are shown here. The data in each row was obtained from Chikaraishi et al. (2009), both Décima et al. (2017) and Décima and Landry (2020), and Bradley et al. (2015), respectively.

	Trophic AAs	Source AAs	β	TDF
$\mathrm{TP_{glu–phe}}$	glutamic acid	phenylalanine	3.4 ± 0.9 ‰	7.1 ± 1.2 ‰
$\mathrm{TP_{ala–phe}}$	alanine	phenylalanine	3.2 ± 1.2 ‰	4.5 ± 2.1 ‰
$\mathrm{TP_{tr–src}}$	gluatamic acid alanine, leucine	glycine, lysine, phenylalanine	2.2 ± 0.7 ‰	6.3 ± 0.9 ‰

trophic amino acids, and glycine, lysine, and phenylalanine as source amino acids, as in Bradley et al. (2015).

An in-situ estimate of trophic position ($\mathrm{TP(in-situ)}$) was also calculated for $\mathrm{TP_{glu–phe}}$, $\mathrm{TP_{ala–phe}}$, and $\mathrm{TP_{tr–src}}$, to account for changes in TP that occurred in particles at the base of the food web. This was calculated by subtracting the mean value for TP of 1-6 μm particles within each depth strata from TP of zooplankton at the same depth. Similarly, the quantity $\Delta\mathrm{TP_{ala–glu}(in-situ)}$ was calculated by subtracting the mean value for $\Delta\mathrm{TP_{ala–glu}}$ of 1-6 μm particles within each depth strata from $\Delta\mathrm{TP_{ala–glu}}$ of zooplankton at the same depth. Uncertainty in TP was calculated by propagating analytical uncertainty associated with the δ^{15}N values of the relevant amino acids, as well as that of β and TDF, as in Jarman et al. (2017) and Ohkouchi et al. (2017). Uncertainty in subsequent calculations of $\Delta\mathrm{TP_{ala–glu}}$, $\mathrm{TP(in-situ)}$, and $\Delta\mathrm{TP_{ala–glu}(in-situ)}$ was estimated using the standard rules for error propagation (Taylor 1997).

To assess the community members responsible for *de novo* synthesis of amino acids at the base of the food web, we used the linear discriminant analysis (LDA) function (*lda*) provided in the MASS package (Ripley et al. 2013). Included in the LDA were δ^{13}C values of six essential amino acids (threonine, valine, leucine, isoleucine, phenylalanine, and lysine), and it was fit using $\delta^{13}\mathrm{C_{EAA}}$ values from various potential source organisms as training data (bacteria, fungi, and microalgae; data from Larsen et al. (2013)). All $\delta^{13}\mathrm{C_{EAA}}$ values included in the LDA were first mean normalized by subtracting the sample's mean $\delta^{13}\mathrm{C_{EAA}}$ value from each of its essential amino acid δ^{13}C values. Inter-laboratory correction factors were applied to all of the data that was collected in the University of Hawaii Biogeochemical Stable Isotope Facility as in Arthur et al. (2014), so that they could be accurately compared with data from Larsen et al. (2013). Using these training data, the LDA was able to identify specific production end-member groups, characterized

by their positions in linear discriminant functional space. Leave one out cross validation was used to assess potential assignment accuracy of the LDA by iteratively running the LDA classification algorithm on training data that was left out of the model fitting procedure. Zooplankton samples were then assigned to an amino acid production end-member using the *predict* function.

Comparisons of any two measured values were assessed using two-tailed t-tests assuming unequal variances. To assess trends across larger portions of the data set, linear models were fit with combinations of depth, size class, tow type (i.e. day or nighttime tow), or sample type (zooplankton, particle, or specific taxa) as predictors, with interactions between predictors allowed whenever multiple predictors were used. The square root transform of depth was often found to minimize residual variance and heteroskedasticity about the regression, and so this transformation was applied when appropriate. ANOVAs were used to assess the significance of predictors and interactions within the linear models.

All statistical analyses were performed in R version 4.0.2 (R Core Team 2018).

3 Results

Contextual oceanographic information is presented in detail in Siegel et al. (2021).

3.1 Source amino acid nitrogen isotopic composition of particles

The two smaller size fractions of particles exhibited large increases in $\delta^{15}N_{SAA}$ values while the larger size fractions did not. Material collected in sediment traps showed low $\delta^{15}N_{SAA}$ values which were similar to those of large particles down to 330 m. The deepest sediment trap sample from 500 m had a slightly higher $\delta^{15}N_{SAA}$ value of 2.1 ± 0.5‰ (Figure 1). The $\delta^{15}N_{SAA}$ values of 0.3-1.0 µm particles collected from 20 to 330 m had the largest range (-2.7±0.1‰ to 10.1±0.4‰), followed by 1-6 µm particles collected from 20 to 500 m (–2.8 ± 0.3‰ to 4.6 ± 0.2‰). The 6-51 and >51 µm particles collected from 20 to 320 m showed much less variation (–1.3 ± 0.4‰ to 1.9 ± 0.5‰; Figure 1). Samples of 1-6 µm particles collected from 0 to 50 m had relatively low $\delta^{15}N_{SAA}$ values (mean: –1.6 ± 0.9‰, range: –2.8 ± 3‰ to –0.5 ± 0.2‰), which were significantly lower than >51 µm particles at these depths (mean: 1.2 ± 0.2‰; t-test, $t = -6.78$, $df = 6$, $p < 0.01$) but not 6-51 µm particles (mean: –0.1 ± 1.8‰; t-test $t = -1.17$, $df = 6$, $p > 0.1$).

The $\delta^{15}N_{SAA}$ values of 6-51 and >51 μm particles did not change significantly below the surface mixed layer (Figure 1; t-test, $t = \text{various}$, $df > 3$, $p > 0.1$), nor did 6-51 and >51 μm particles collected at 320 m differ from one another (t-test, $t = 0.22$, $dof = 4$, $p > 0.1$), with all particles >6 μm collectively having an average $\delta^{15}N_{SAA}$ value of $0.9 \pm 0.7‰$ at 320 m. The $\delta^{15}N_{SAA}$ values of 1-6 μm particles, on the other hand, increased rapidly with depth from an average value of $-1.6 \pm 0.9‰$ in the mixed layer to an average of $3.8 \pm 0.6‰$ below 300 m (Figure 1). The $\delta^{15}N_{SAA}$ values of 0.3-1.0 μm particles increased even more rapidly with depth from an average value of $-2.4 \pm 0.5‰$ in the mixed layer to an average of $8.6 \pm 2.1‰$ below 300 m (Figure 1). The $\delta^{15}N_{SAA}$ values of both 0.3-1.0 and 1-6 μm particles showed significant linear relationships with the square root of depth (0.3-1.0 μm: ANOVA, $F_{1,3} = 59.91$, $p < 0.01$; 1-6 μm: ANOVA, $F_{1,18} = 48.63$, $p < 0.001$). The $\delta^{15}N_{SAA}$ values of all particle size classes overlap from 85 m to 155 m, however at and below 195 m the $\delta^{15}N_{SAA}$ values of <6 μm particles became significantly higher that those of both >6 μm particles collected and sediment trap material at all depths (t-test, $t = \text{various}$, $df > 3$, $p < 0.05$).

3.2 Source amino acid nitrogen isotopic composition of the zooplankton community

The $\delta^{15}N_{SAA}$ values of zooplankton from the 0.2-0.5 and 1-2 mm size fractions of nighttime tows (Figure 2a,b) ranged from $-0.2 \pm 0.3‰$ to $6.3 \pm 0.3‰$, and both size classes showed highly significant linear relationships with the square root of depth below 50 m (ANOVA, $F_{1,1,1,14} = 47.51$, $p =< 0.001$), which were independent of zooplankton size (size effect: ANOVA, $F_{1,1,1,14} = 1.19$, $p > 0.1$; size-depth interaction: ANOVA, $F_{1,1,1,14} = 0.10$, $p > 0.1$). The 0.2-0.5 and 1-2 mm zooplankton collected in the 0-50 m depth strata had $\delta^{15}N_{SAA}$ values which were higher than those of large particles collected at the same depth (0.2-0.5 mm zooplankton: t-test, $t = 4.10$, $dof = 7$, $p < 0.05$; 1-2 mm zooplankton: t-test, $t = 5.23$, $dof = 7$, $p < 0.01$), while below 50 m zooplankton in these size classes showed depth dependent trends in $\delta^{15}N_{SAA}$ which are visually similar to those of the 1-6 μm particles (Figure 2a,b). The $\delta^{15}N_{SAA}$ values of 0.2-0.5 mm zooplankton below 50 m were not statistically different from 1-6 μm particles (ANOVA, $F_{1,1,1,23} = 3.77$, $p > 0.05$). The 1-2 mm zooplankton had a distinct relationship with depth

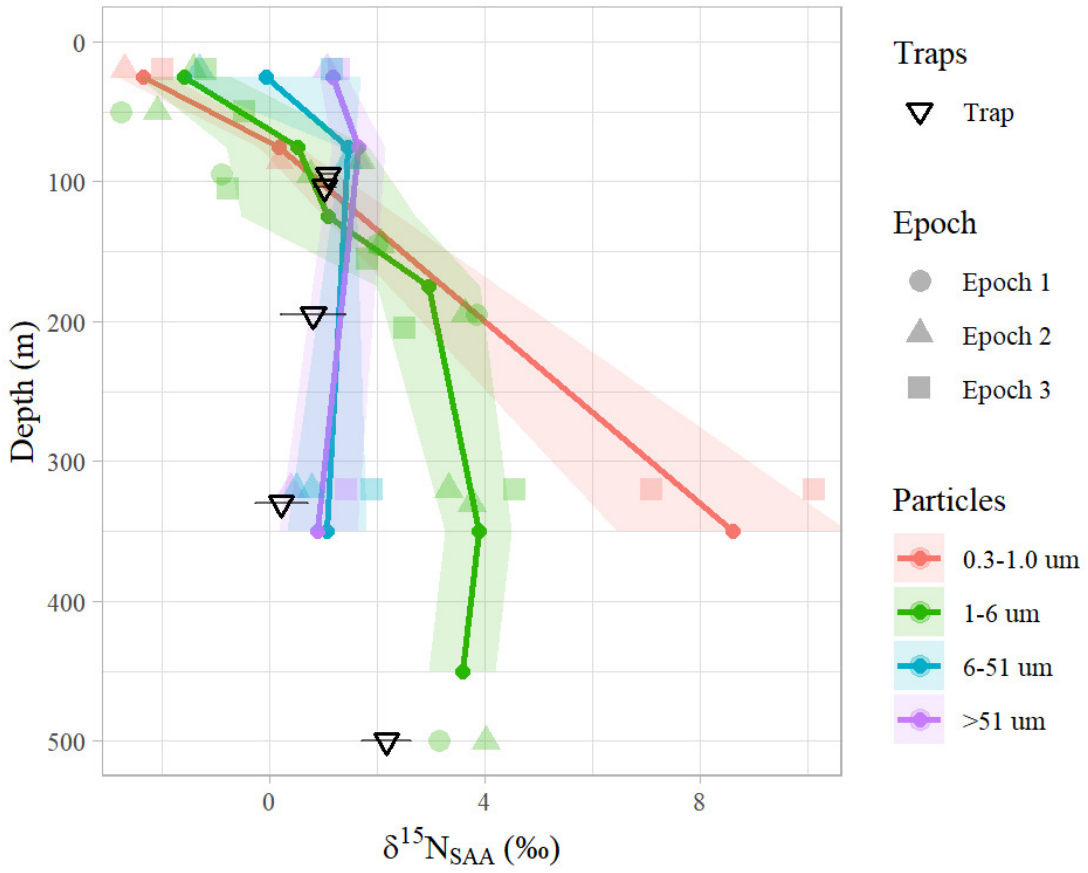

Figure 1: The $\delta^{15}N_{SAA}$ values of particles plotted as a function of depth. Samples of particles collected by in-situ filtration are shown in transparent shapes, with size classes differentiated by color and the collection epoch by shape. The solid points and lines describe the average $\delta^{15}N_{SAA}$ values when samples are binned into depth strata, with the shaded ribbons around each line describing the propagated standard deviation associated with each average value. Depth strata were chosen to be consistent with those used for zooplankton collection. Sediment trap samples are shown as upside down triangles.

(ANOVA, $F_{1,1,1,23} = 5.04$, $p < 0.05$), with their $\delta^{15}N_{SAA}$ value increasing more rapidly with depth through the upper mesopelagic zone than those of 1-6 μm particles. 0.2-0.5 and 1-2 mm zooplankton had an average nighttime $\delta^{15}N_{SAA}$ value below 200 m of 4.0 ± 0.1‰ and 4.6 ± 0.1‰, respectively.

The $\delta^{15}N_{SAA}$ value of the 2-5 mm zooplankton (Figure 2c) ranged from 1.0 ± 0.2‰ to 4.3 ± 0.4‰ and showed a significant linear relationship with depth (ANOVA, $F_{1,2} = 61.40$, $p < 0.05$), increasing constantly from the lower euphotic zone into the deep mesopelagic. They had a $\delta^{15}N_{SAA}$ value similar to >51 μm particles in the mixed layer (t-test, $t = 1.54$, $dof = 7$, $p > 0.1$) that decreased in the lower euphotic zone becoming similar to 1-6 μm particles (t-test, $t = 0.67$, $dof = 4$, $p > 0.1$). Below the euphotic zone their $\delta^{15}N_{SAA}$ value increased consistently with depth, though it was still 1.1‰ lower than that of 1-6 μm particles at 350 m. The $\delta^{15}N_{SAA}$ value of >5 mm zooplankton (Figure 2d), on the other hand, was lower than that of >6 μm particles in the mixed layer and ranged from 0.3 ± 0.2‰ to 3.8 ± 0.2‰ throughout the water column. Their $\delta^{15}N_{SAA}$ value increased linearly from the mixed layer into the upper mesopelagic zone (ANOVA, $F_{1,1} = 388.68$, $p < 0.05$; Figure 2d) where it was not different from those of the 1-6 μm particles (t-test, $t = –0, 1$, $dof = 4$, $p > 0.1$).

$\delta^{15}N_{SAA}$ values for 0.2-0.5 and 1-2 mm size classes of zooplankton collected during the daytime in the mesopelagic were significantly lower in than those collected at night (Figure 2e,f; t-test, $t =$ various, $dof = 4$, $p < 0.05$), with the exception of 150-200 m and 400-500 m (t-test, $t =$ various, $dof = 4$, $p > 0.1$). The $\delta^{15}N_{SAA}$ values in mesopelagic samples ranged from 2.4 ± 0.2‰ to 3.5 ± 0.3‰ with a mean of 3.0 ± 0.5 ‰. The $\delta^{15}N_{SAA}$ values of 0.2-0.5 mm zooplankton collected in daytime and nighttime tows were significantly different from one another at all measured depths (t-test, $t =$ various, $dof = 4$, $p < 0.05$) except 150-200 and 400-500 m (t-test, $t =$ various, $dof = 4$, $p > 0.1$), with the nighttime community tending to have higher $\delta^{15}N_{SAA}$ values than the daytime community in the euphotic zone, and lower $\delta^{15}N_{SAA}$ values in the mesopelagic. The $\delta^{15}N_{SAA}$ values of 1-2 mm zooplankton collected in daytime and nighttime tows were significantly different from one another at all depths (t-test, $t =$ various, $dof = 4$, $p < 0.01$), except for 150-200 m (t-test, $t = 0.05$, $dof = 4$, $p > 0.1$). For both size classes, tow type (i.e. day versus night) was found to have a significant effect on the linear relationship observed between $\delta^{15}N_{SAA}$ values and the square root of depth (0.2-0.5 mm zooplankton: ANOVA, $F_{1,1,1,11} = 5.61$,

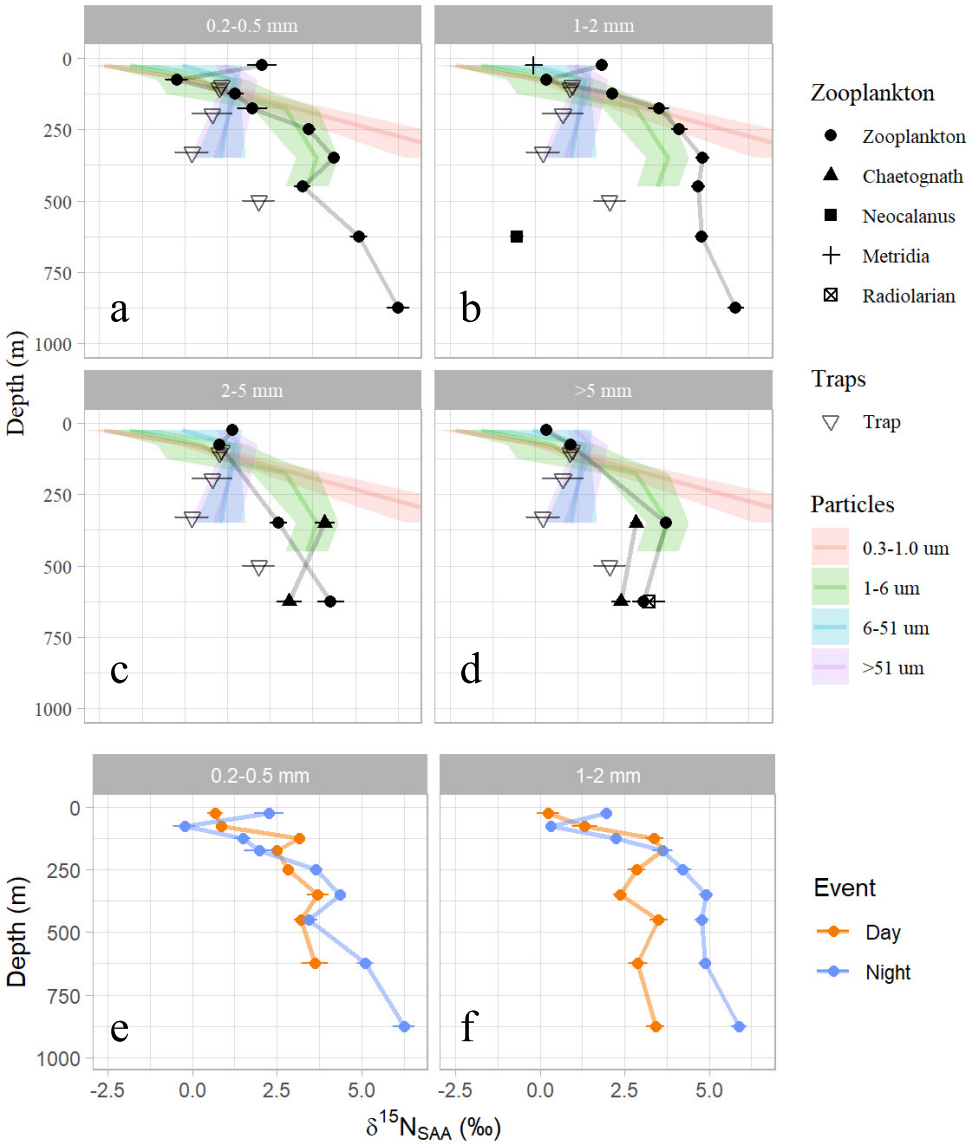

Figure 2: Particles and zooplankton$\delta^{15}N_{SAA}$ values plotted as a function of depth. Panels **a-d** show the cruise average $\delta^{15}N_{SAA}$ values of 0.3-1.0, 1-6, 6-51, and >51 µm particles binned by depth, with line color differentiating particle size class. Sediment trap material is plotted as open upside down triangles. Each panel shows the $\delta^{15}N_{SAA}$ values of a specific size class of zooplankton, as indicated in the panel title, all collected in a single nighttime MOCNESS tow (tow 89). Types of zooplankton within each size class are indicated by shapes with the whole community shown as circles, chaetognaths as triangles, *Neocalanus spp.* as squares, *Metridia spp.* as crosses, and radiolaria as crossed squares. Panels **e** and **f** show a comparison of $\delta^{15}N_{SAA}$ values for select zooplankton size fractions collected in daytime and nighttime MOCNESS tows, with the daytime tows shown in orange and the nighttime tows in blue. 0.2-0.5 and 1-2 mm zooplankton had average nighttime $\delta^{15}N_{SAA}$ values below 200 m of 4.0 ± 0.1‰ and 4.6 ± 0.1‰, and daytime $\delta^{15}N_{SAA}$ values below 200 m of 3.3 ± 0.1‰ and 3.0 ± 0.1‰, respectively.

$p < 0.05$; 1-2 mm zooplankton: ANOVA, $F_{1,1,1,11} = 7.92$, $p < 0.05$). 0.2-0.5 and 1-2 mm zooplankton had average daytime $\delta^{15}N_{SAA}$ values below 200 m of $3.3 \pm 0.1‰$ and $3.0 \pm 0.1‰$ respectively.

3.3 Source amino acid nitrogen isotopic composition of specific taxa

Calanoid copepods of the genera *Neocalanus* (size: 1-2 mm; depth: 500-750 m; ontogenetic migrator) and *Metridia* (size: 1-2 mm; depth: 0-50 m; diel vertical migrator) were isolated from nighttime tows and found to have similar $\delta^{15}N_{SAA}$ values that were lower than the rest of the nighttime zooplankton community (Figure 2b). The $\delta^{15}N_{SAA}$ value of *Neocalanus spp.* was not statistically different from 1-6 μm particles collected above 50 m (t-test, $t = 2.61$, $dof = 6$, $p > 0.05$), and the $\delta^{15}N_{SAA}$ value of *Metridia spp.* was similar to the mean of all mixed layer particles.

Three out of four of the chaetognath samples analyzed (size: 2-5 and >5 mm; depth: 300-400 & 500-750 m; nighttime tows) had $\delta^{15}N_{SAA}$ values lower than the other nighttime zooplankton community samples from the same depths (Figure 2c,d). The fourth chaetognath sample had a $\delta^{15}N_{SAA}$ value which was not significantly different from those of 1-6 μm small particles in the 300-400 m range (t-test, $t = 0.58$, $dof = 4$, $p > 0.1$). When the $\delta^{15}N_{SAA}$ values of chaetognaths (2-5 and >5 mm size classes) were averaged within the 300-400 and 500-750 m depth strata we found no significant difference between the $\delta^{15}N_{SAA}$ values of chaetognaths and daytime zooplankton (0.2-0.5 and 1-2 mm size classes) at either depth (300-400 m: t-test, $t = 2.72$, $dof = 2$, $p > 0.1$; 500-750 m: t-test, $t = -2.00$, $dof = 2$, $p > 0.1$).

Radiolaria (>5 μm) from day and nighttime tows were found to have $\delta^{15}N_{SAA}$ values (Figure 2e,f) that were not significantly different from one another (t-test, $t = 0.33$, $dof = 4$, $p > 0.1$), or from the average daytime community at 500-750 m (nighttime radiolaria: t-test, $t = 0.21$, $dof = 4$, $p > 0.1$).

3.4 Source amino acid nitrogen isotope mass balance mixing models

When small (1-6 μm) and large (>51 μm) particle $\delta^{15}N_{SAA}$ values were used as mixing model end members to assess the fractional contributions of small particles to the base of the zooplankton

Table 2: End member $\delta^{15}N_{SAA}$ values for the two component $\delta^{15}N_{SAA}$ mixing model are tabulated. 1-6 μm particles were used for the small particle end member and >51 μm particles were used for the large particle end member. At depths where samples were not available, end member $\delta^{15}N_{SAA}$ values were estimated by linear interpolation using samples collected at adjacent depths. These values are indicated with *.

Depth	small (1-6 μm)	large (>51 μm)
25 m	-1.6 ± 0.3‰	1.2 ± 0.3‰
75 m	0.5 ± 1.3‰	1.6 ± 0.5‰
125 m	1.1 ± 1.6‰	1.5 ± 0.5‰*
175 m	2.9 ± 1.0‰	1.4 ± 0.6‰*
250 m	3.3 ± 0.8‰*	1.2 ± 0.6‰*
350 m	3.9 ± 0.6‰	0.9 ± 0.7‰
450 m	3.6 ± 0.6‰	0.9 ± 0.7‰*

food web (Table 2), we found that small particles were the dominant source of material to the base of the mesopelagic zooplankton food web. For whole zooplankton community samples, fractional contributions of small particles (f_{small}) ranged from -0.39 ± 0.14 to 1.66 ± 0.15, however, values <0 and >1 were set to 0 and 1 for reporting (Table 3) and subsequent analyses. For zooplankton in the top 50 m we found $f_{small} \approx 0$, with >5 mm zooplankton being the only size class to give $f_{small} > 0$ (Table 3). At 50-100 m, however, $f_{small} = 1$ for the 0.2-0.5 and 1-2 mm zooplankton while the 2-5 and >5 mm zooplankton had values that were intermediate (0.54 ± 0.4 and 0.54 ± 0.39 respectively). Throughout the upper mesopelagic $f_{small} \approx 1$ for 0.2-0.5, 1-2, and >5 mm zooplankton, while 2-5 mm zooplankton had $f_{small} = 0.62 \pm 0.10$. When mixing model results were averaged across size classes and depth strata, and were weighted by cruise average biomass, the average small particle contribution was higher in the mesopelagic ($f_{small} = 0.84 \pm 0.12$) than in the top 100 m ($f_{small} = 0.22 \pm 0.15$).

When used for samples of specific taxa, the small/large particle-based $\delta^{15}N_{SAA}$ mixing model produced values of f_{small} ranging from -0.53 ± 0.25 to 1.35 ± 0.31 (Table 4). The 1-2 mm *Neocalanus spp.* captured at 500-750 m were the only sample to produce a negative value (-0.53 ± 0.25). *Metridia spp.* had the highest f_{small} of any sample measured in the 0-50 m depth strata ($f_{small} = 0.44 \pm 0.09$‰) while the >5 mm chaetognaths from 500-750 m had the lowest f_{small} of any sample measured in the mesopelagic ($f_{small} = 0.60 \pm 0.12$‰).

Table 3: Two component $\delta^{15}N_{SAA}$ mixing model results for size fractionated zooplankton community samples are tabulated by depth and by size class. Large and small particle end member are defined as >51 and 1-6 μm particles respectively. Mean values of f_{small} within a size class are given for specific depth ranges in the bottom three rows, and within each depth in the right two columns. Proportions of whole community biomass attributed to each size fraction at each depth were averaged over the duration of the cruise and used as weighting factors to calculate the biomass weighted averages. The 0.5-1.0 mm size class was included in community averages by assuming its mixing model results could be accurately represented as the mean of the 0.2-0.5 and 1-2 mm size class. Values of $f_{small} < 0$ or $f_{small} > 1$ have been set to 0 and 1 respectively.

Depth	0.2-0.5 mm f_{small}	1-2 mm f_{small}	2-5 mm f_{small}	>5 mm f_{small}	Average f_{small}	Biomass Weighted Average f_{small}
0 - 50 m	0.00±0.14	0.00±0.09	0.00±0.07	0.31±0.07	0.08±0.05	0.04±0.05
50 - 100 m	1.00±1.15	1.00±0.79	0.54±0.40	0.54±0.39	0.77±0.38	0.66±0.33
200 - 300 m	1.00±0.25	1.00±0.32	–	–	–	–
300 - 400 m	1.00±0.14	1.00±0.17	0.62±0.10	0.98±0.12	0.90±0.07	0.83±0.28
400 - 500 m	1.00±0.15	1.00±0.21	–	–	–	–
Average (all depths)	0.83±0.31	0.83±0.23	0.54±0.12	0.67±0.11	0.68±0.10	**0.55±0.28**
Average (0-100 m)	0.50±0.29	0.50±0.20	0.27±0.10	0.43±0.10	0.42±0.09	**0.22±0.15**
Average (200-500 m)	1.00±0.11	1.00±0.14	0.62±0.10	0.98±0.12	0.90±0.07	**0.84±0.12**

Table 4: Two component $\delta^{15}N_{SAA}$ mixing model results for taxon specific samples are tabulated by depth and taxa. Large and small particle end member are defined as >51 and 1-6 μm particles respectively.

Size, Taxa	0-50 m f_{small}	300-400 m f_{small}	500-750 m f_{small}
1-2 mm, Metridia	0.44±0.09	–	–
1-2 mm, Neocalanus	–	–	-0.53±0.25
2-5 mm, Chaetognatha	–	1.35±0.31	0.81±0.14
>5 mm, Chaetognatha	–	0.82±0.18	0.60±0.12
>5 mm, Radiolaria	–	–	0.95±0.13

3.5 Particle trophic position

All estimates of particle trophic position showed significant positive linear relationships with the square root of depth (Figure 3a,b; ANOVA, $F_{4,1,3,28} = \text{various}$, $p < 0.001$). $TP_{glu–phe}$ and $TP_{ala–phe}$ increased from average values of 1.2±0.3 and 1.2±0.4 in the mixed layer to 1.8±0.4 and 2.5±0.5 below 300 m, respectively. The difference between $TP_{ala–phe}$ and $TP_{glu–phe}$ at each depth ($\Delta TP_{ala–glu}$; Figure 7d; mean: 0.3 ± 0.4, range: -0.3 ± 0.4 to 1.2 ± 1.0) was not found to be significantly different from 0 (Figure 7; t-test, $t = \text{various}$, $dof = 4$, $p > 0.1$), however the choice of amino acids (i.e. glu and phe vs. ala and phe) was found to be a significant predictor of TP in linear models (ANOVA, $F_{1,1,1,70} = 48.06$, $p < 0.001$), with the effect being strongest in the mesopelagic zone. Particle size was found to be a significant predictor of $TP_{glu–phe}$ in linear models (ANOVA, $F_{4,1,3,28} = 6.85$, $p < 0.001$), with larger particles tending to have a higher TP, but this was only marginally significant for $TP_{ala–phe}$ (ANOVA, $F_{4,1,3,28} = 2.48$, $p < 0.1$).

3.6 Zooplankton trophic position

Samples of the whole zooplankton community collected in nighttime tows had a higher $TP_{glu–phe}$ (mean: 2.8 ± 0.3, range: 2.1 ± 0.3 to 3.4 ± 0.4) than particles at nearly all depths (Figure 3a; t-test, $t = \text{various}$, $p < 0.05$). Zooplankton $TP_{glu–phe}$ did not show a significant relationship with depth (ANOVA, $F_{1,3,3,18} = 0.25$, $p > 0.1$), but $TP_{glu–phe}$ increased with size (ANOVA, $F_{1,3,3,18} = 3.94$, $p < 0.05$). Values obtained for $TP_{tr–src}$ followed similar trends (data not shown).

$TP_{ala–phe}$ was found to be higher than $TP_{glu–phe}$ for all zooplankton samples, with the difference between the two ($\Delta TP_{ala–glu}$) ranging from 1.1 ± 1.3 to 2.2 ± 1.9 with a mean of 1.6 ± 0.3. $\Delta TP_{ala–glu}$ was not found to be significantly different from zero for any one individual sample, but when the mean $\Delta TP_{ala–glu}$ was calculated along with its propagated uncertainty within each depth strata (Figure 7b), mean $\Delta TP_{ala–glu}$ was found to be significantly greater than 0 throughout 70% of the water column (depths: 0-50, 50-100, 300-400, 500-750, and 750-1000 m; t-test, $t = \text{various}$, $dof = 6$, $p < 0.5$) and not in the remainder (depths: 100-150, 150-200, 200-300, 400-500; t-test, $t = \text{various}$, $dof = 6$, $p < 0.1$). Size was not found to have a significant effect on $\Delta TP_{ala–phe}$ (ANOVA, $F_{1,3,3,18} = 1.57, p > 0.1$).

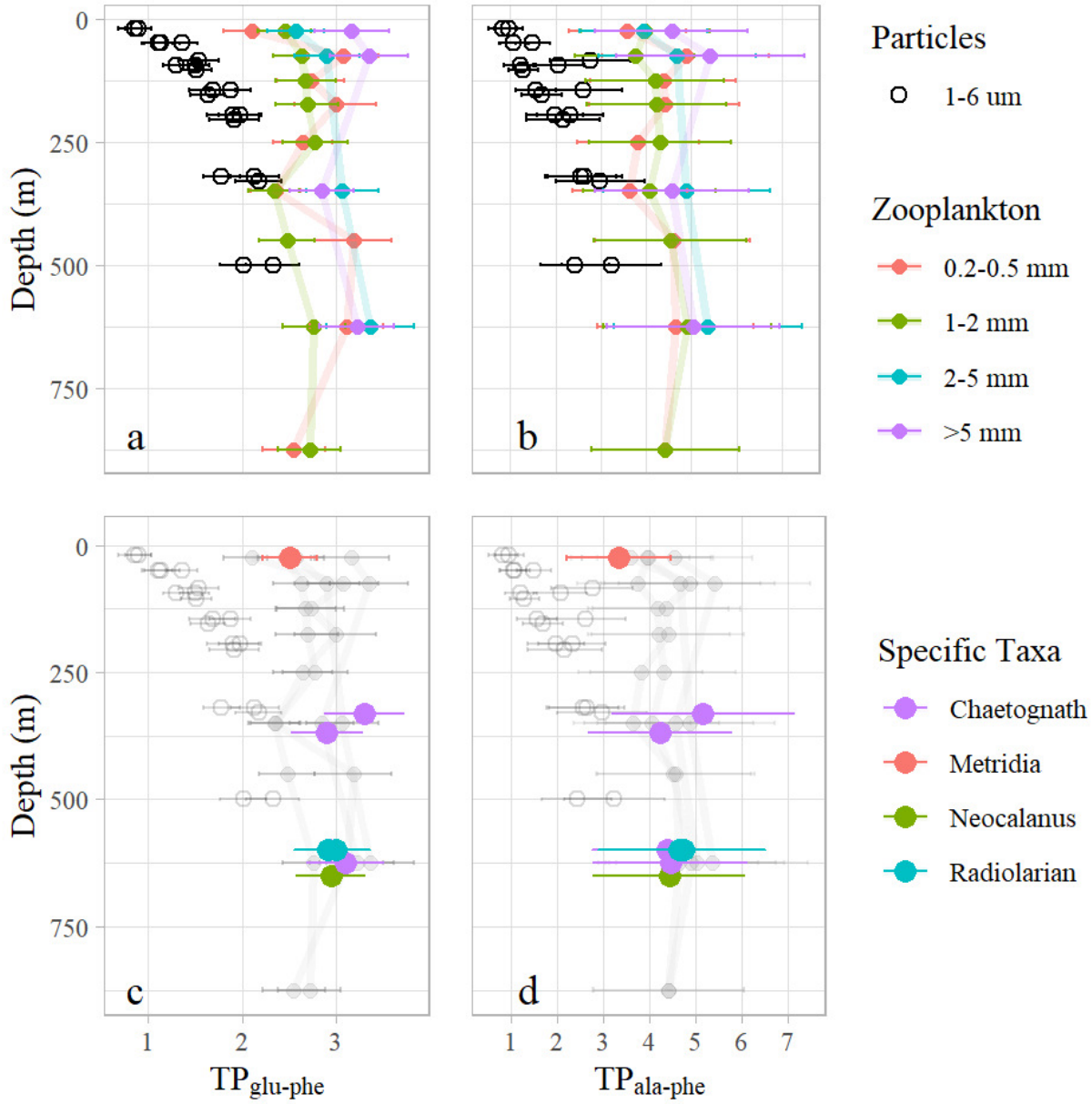

Figure 3: $\mathrm{TP_{glu-phe}}$ and $\mathrm{TP_{ala-phe}}$ for zooplankton and particles is plotted against depth. Panels **a** and **b** show $\mathrm{TP_{glu-phe}}$ and $\mathrm{TP_{ala-phe}}$, respectively for particles and size fractionated zooplankton community samples. 1-6 µm particles are shown in open black circles, while zooplankton are shown in lines and points with colors differentiating size classes. Error bars indicate the propagated standard deviation associated with each sample. Panels **c** and **d** show $\mathrm{TP_{glu-phe}}$ and $\mathrm{TP_{ala-phe}}$ plotted similarly for specific taxa, with colors differentiating different taxa.

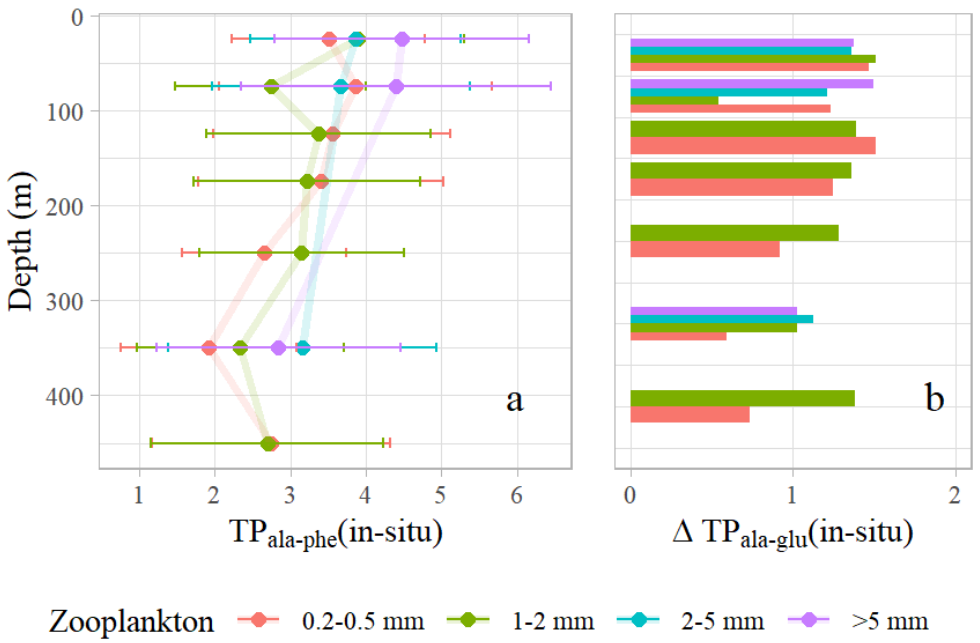

Figure 4: $\mathrm{TP_{ala-phe}(in-situ)}$ and $\Delta\mathrm{TP_{ala-glu}(in-situ)}$ for size fractionated zooplankton community samples is plotted against depth. Panel **a** shows $\mathrm{TP_{ala-phe}(in-situ)}$ and **b** shows $\Delta\mathrm{TP_{ala-glu}(in-situ)}$. Both quantities have been adjusted such that 1-6 µm particles are set to $\mathrm{TP_{ala-phe}} = 1$ or $\Delta\mathrm{TP_{ala-glu}} = 0$. Colors differentiate size classes of zooplankton, and error bars indicate the propagated standard deviation associated with each sample. Error bars are omitted from panel **b** for clarity.

When $\mathrm{TP_{ala–phe}}$ of particles was subtracted from that of zooplankton within each depth to obtain $\mathrm{TP_{ala–phe}(in-situ)}$ (Figure 4a), the resulting estimate of trophic position ranged from 1.9 ± 1.2 to 4.5 ± 1.7, and a significant, negative linear relationship with depth was observed (ANOVA, $\mathrm{F_{1,3,3,12}} = 26.04$, $\mathrm{p} < 0.001$). While zooplanton size was not found to be a significant predictor of $\mathrm{TP_{ala–glu}(in-situ)}$, 0.2-0.5 or 1-2 mm zooplankton were consistently observed to have the lowest trophic position at a given sampling depth, while 2-5 or >5 mm zooplankton were observed to have the highest, with the range in zooplankton $\mathrm{TP_{ala–glu}(in-situ)}$ often being >1 (Figure 4). When zooplankton data was aggregated into small (0.2-0.5 and 1-2 mm) and large (2-5 and >5 mm) size classes and $\mathrm{TP_{glu–phe}(in-situ)}$ was compared within a given sampling depth, estimates of trophic position ranged from 1.3 ± 0.2 to 3.1 ± 0.4. Again, a significant, negative linear relationship with depth was observed (ANOVA, $\mathrm{F_{3,1,3,12}} = 33.05$, $\mathrm{p} < 0.001$), and zooplankton size *was* found to be a significant predictor of $\mathrm{TP_{glu–phe}(in-situ)}$ (ANOVA, $\mathrm{F_{3,1,3,12}} = 5.05$, $\mathrm{p} < 0.02$). $\mathrm{\Delta TP_{ala–glu}(in-situ)}$ was not found to be significantly greater than zero for any particular size class, but when the mean $\mathrm{\Delta TP_{ala–glu}(in-situ)}$ was calculated within each depth strata and the error propagated, mean $\mathrm{\Delta TP_{ala–glu}(in-situ)}$ was significantly greater than zero at some depths (0-50 m, 50-100 m, 100-150 m, 300-400 m; t-test, $\mathrm{f} =$ various, $\mathrm{p} < 0.05$) and not at others (150-200 m, 200-300 m, 400-500 m; t-test, $\mathrm{f} =$ various, $\mathrm{p} > 0.05$). $\mathrm{\Delta TP_{ala–glu}(in-situ)}$ was found to have a significant negative linear relationship with depth (ANOVA, $\mathrm{F_{1,18}} = 5.4$, $\mathrm{p} < 0.05$)

The trophic position of specific taxa are summarized in Table 5.

Table 5: $\mathrm{TP_{glu–phe}}$ and $\mathrm{TP_{ala–phe}}$ for specific taxa are tabulated here.

	$\mathrm{TP_{glu–phe}}$			$\mathrm{TP_{ala–phe}}$		
Size, Taxa	0-50 m	300-400 m	500-750 m	0-50 m	300-400 m	500-750 m
1-2 mm, Metridia	2.5 ± 0.3	–	–	3.3 ± 1.2	–	–
1-2 mm, Neocalanus	–	–	4.9 ± 0.4	–	–	4.4 ± 1.6
2-5 mm, Chaetognatha	–	2.9 ± 0.5	3.1 ± 0.4	–	4.3 ± 1.5	4.5 ± 1.7
>5 mm, Chaetognatha	–	3.3 ± 0.4	2.9 ± 0.4	–	5.2 ± 2.0	4.4 ± 1.6
>5 mm, night, Radiolaria	–	–	3.0 ± 0.4	–	–	4.7 ± 1.8
>5 mm, day, Radiolaria	–	–	2.9 ± 0.4	–	–	4.9 ± 1.8

3.7 Zooplankton essential amino acid carbon isotopic fingerprinting

The δ^{13}C values of all essential amino acids in nighttime collected zooplankton ranged from -33.4 ± 0.4‰ to -6.9 ± 0.6‰ with a mean and standard deviation of -24.3 ± 6.7‰. The average EAA δ^{13}C value of each zooplankton sample ranged from -25.8‰ to -22.0‰ with a mean and standard deviation of -24.3 ± 1.2‰. There was no significant trend in mean EAA δ^{13}C with depth (ANOVA, $\mathrm{F}_{1,24} = 0.15$, $\mathrm{p} > 0.1$) nor was there any effect of depth on any EAA's δ^{13}C value except for lysine (ANOVA, $\mathrm{F}_{1,24} = 5.6$, $\mathrm{p} < 0.05$), though the effect size was small.

When we fit an LDA using mean normalized $\delta^{13}\mathrm{C}_{\mathrm{EAA}}$ values for all of the available training data (microalgae, macroalgae, seagrass, terrestrial plants, fungi, and bacteria), leave one out cross validation indicated a 85% classification accuracy, with the bulk of classification errors attributed to the inability to separate macroalgal, microalgal, and seagrass end members. When used to classify our zooplankton data set, 25 of the 26 zooplankton samples used were assigned to the microalgal end member and one was assigned to macroalgae. Removing some end members that are unrealistic for OSP (macroalgae, seagrass, terrestrial plants) resulted in 100% classification accuracy as estimated by leave one out cross validation. Using this model to classify zooplankton assigned all zooplankton to the microalgal end member with >99.9% certainty (Figure 5a).

Bacterial and microalgal end members are largely distinguished based on LD2, which accounts for 38% of the variation in the training data set. When the 750-1000 m sample is excluded, we find that depth is a significant predictor of LD2 (Figure 5b, ANOVA, $\mathrm{F}_{1,22} = 6.68$, $\mathrm{p} < 0.05$), though the effect size is small with LD2 variation in the zooplankton data set making up roughly 10% variation in the whole training data set. The fungal end member is distinguished from microalagal and bacterial end members based on LD1, which accounts for 62% of the variation in the training data set. LD1 shows a weak and non-significant trend to lower values with depth (Figure 2c; ANOVA, $\mathrm{F}_{1,24} = 1.44$, $\mathrm{p} > 0.1$), with values generally consistent with microalgae and bacteria.

4 Discussion

Constraining how mesopelagic zooplankton communities interact with sinking particles is central to building our understanding of how zooplankton affect the marine carbon cycle. Furthermore, understanding food web linkages allows us to evaluate what pathways are important in supplying

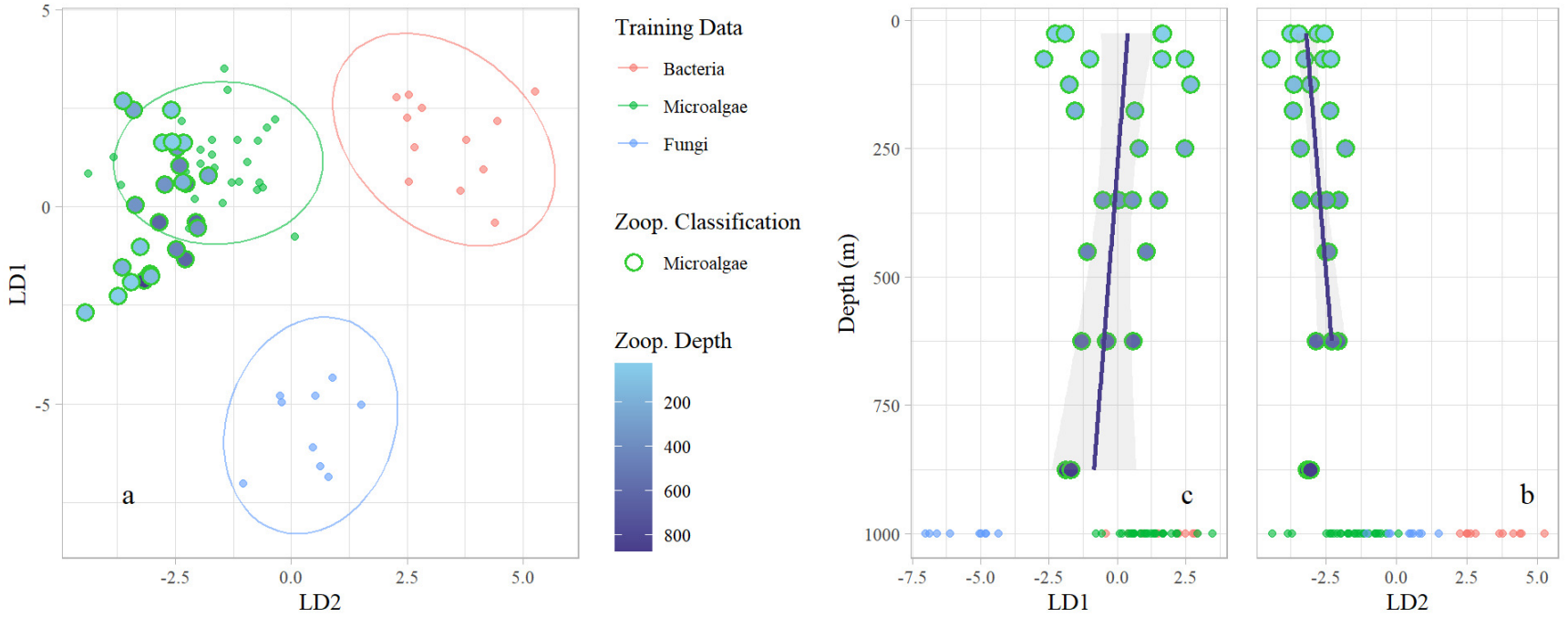

Figure 5: Results from linear discriminant analysis of mean normalized $\delta^{13}C_{EAA}$ values of size fractionated zooplankton community samples, where literature bacteria, fungi, and microalgae were used as training data. Panel **a** shows a biplot of linear discriminant functions 1 and 2, which account for 62% and 38% of variation in the training data, respectively. Those training data are plotted in small points colored by end member designation, with ellipses indicating the 95% confidence interval assuming a multivariate t-distribution. Zooplankton data classified using these linear discriminant functions are shown in larger circles, where the outer color corresponds to their assigned end member group and the inner color corresponds to their depth of collection. Panels **b** and **c** show LD2 and LD1 plotted as a function of depth for the same data, with literature end members shown at 1000 m. Linear regressions are plotted in dark blue with the 95% confidence interval indicated with the shaded region about the regression line.

energy to deep sea food webs. This study focused on both of these topics, asking generally: How is the mesopelagic zooplankton food web structured? and specifically: to what degree do small particles, large particles, and actively transported materials compose the base of the mesopelagic zooplankton food web? Answers to these questions help address EXPORTS Science Question 2 (Siegel et al. 2015) "What controls the efficiency of vertical transfer of organic matter below the well-lit surface ocean?" Here we find strong evidence indicating that the base of the mesopelagic zooplankton food web is composed mainly of <6 μm particles, suggest that mesopelagic zooplankton feed predominantly on resident zooplankton with the exception of predatory zooplankton >2 mm which derive a portion of their diet from carnivory of vertically migrating individuals at depth, and provide compelling evidence that prostistan heterotrophs are an important trophic intermediary down to at least 500 m.

4.1 Assessing the importance of small particles to the mesopelagic zooplankton food web

To understand how the zooplankton community affects sinking particle flux in the mesopelagic zone, one goal of this study was to characterize the base of the mesopelagic zooplankton food web at OSP. Central to this goal was to determine the size of particles that form the base of that food web. This assessment was made possible by the presence of two standing stocks of particle (larger and smaller than 6 μm) which had characteristically different $\delta^{15}N_{SAA}$ values at and below 195 m (Figure 1). This is similar to what has been documented elsewhere in the North Pacific (Hannides et al. 2013, 2020; Yamaguchi and McCarthy 2018; Romero-Romero et al. 2020). As found in these related studies, the relative importance of these distinct stocks of particulate material to the zooplankton food web could be quantified using a simple two-end member $\delta^{15}N_{SAA}$ mass balance mixing model (Tables 3 and 4).

Small zooplankton (0.2-0.5, 0.5-1.0, and 1-2 mm size fractions) made up $35 \pm 5\%$ of the mesopelagic biomass collected at OSP (Figure 6) and mixing model results indicated the average proportion of small particles (f_{small}) making up the base of the 0.2-0.5 and 1-2 mm zooplankton food webs in the upper mesopelagic zone was $100 \pm 11\%$ and $100 \pm 14\%$ respectively (Table 3). This result is a clear indication that particles smaller than 6 μm were the primary resource

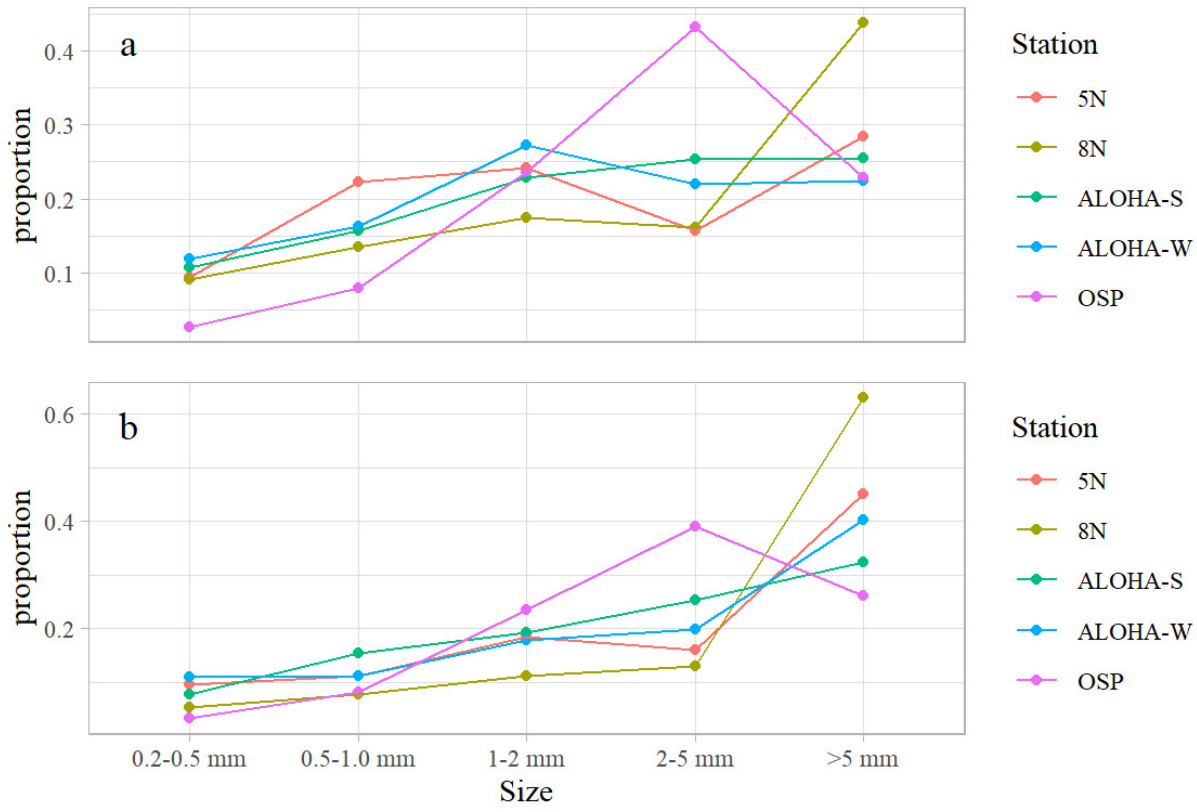

Figure 6: Fractional contributions of zooplankton size classes to total biomass integrated over different depth ranges are compared, with stations indicated by color. Panel **a** reflects relative contributions of zooplankton size classes integrated from 0-1000 m, while panel **b** indicates biomass integrated from 200-1000 m.

constituting the base of the mesopelagic 0.2-2 mm zooplankton food web. The $\delta^{15}N_{SAA}$ values of many 1-2 mm zooplankton in the mesopelagic were even higher than those of 1-6 µm particles (Figure 2,b). This suggests that the 1-2 mm zooplankton food web is based in part on either $<$1 µm particles, or a subset of the 1-6 µm particle size class with a higher $\delta^{15}N_{SAA}$ value than the average.

Large zooplankton (2-5 and $>$5 mm) accounted for $65 \pm 17\%$ of zooplankton biomass collected at OSP (Figure 6), and generally had lower $\delta^{15}N_{SAA}$ values compared to 0.2-0.5 and 1-2 mm zooplankton, as well as particles in the 1-6 µm size fraction in the mesopelagic (Figure 2c,d). Mixing model results indicated that the food web base for 2-5 and $>$5 mm zooplankton in the upper mesopelagic was composed of $62 \pm 0.10\%$ and $98 \pm 0.12\%$ small particles respectively (Table 3). While this does give some indication that materials other than small particles contribute in part to

resource supply in the region, it supports the fact that small particles form the majority of the food web base in the upper mesopelagic, with the zooplankton biomass weighted average contribution of small particles for all zooplankton size classes estimated to be 84±0.12%.

It is well established that active transport by vertical migration of zooplankton can also be responsible for a significant flux of organic material into the mesopelagic via grazing near the surface and fecal pellet production or predator-prey interactions at depth (Steinberg et al. 2000). In fact, we find evidence that larger predatory taxa do appear to be sourcing some portion of their diet from vertical migrators at depth. Our two-end member mixing model, however, estimates $\mathrm{f_{small}}$ by assuming that large and small passively sinking particles represent the only two possible sources of material to the zooplankton food web, with the importance of large particles being identified by their lower $\delta^{15}\mathrm{N_{SAA}}$ values. However, $\delta^{15}\mathrm{N_{SAA}}$ values of presumed vertical migrators such as *Metridia spp.* and *Neocalanus spp.* were also low, which is characteristic of "fresh" surface-derived material (Figure 2b). As a result, predation of these vertically migrating zooplankton could also impart lower $\delta^{15}\mathrm{N_{SAA}}$ values to predatory mesopelagic zooplankton. Evidence for this will be addressed in more detail in the following section, but here it is worth noting that because vertical migrators have $\delta^{15}\mathrm{N_{SAA}}$ values which are even lower than those of large particles in the mesopelagic (Figure 2b), their exclusion from mixing models could only result in an underestimation of $\mathrm{f_{small}}$. This would not change the major finding that small particles make up the majority of the base of the zooplankton food web in the upper mesopelagic zone.

The finding that the supply of organic material to the mesopelagic food web was dominated by particles smaller than 6 μm at OSP and elsewhere (Romero-Romero et al. 2020) suggests that at some locations they represent an ecologically important source of carbon. Moreover, this material appears to not be recorded in sediment traps, as evidenced by their low $\delta^{15}\mathrm{N_{SAA}}$ values. Whether or not their flux is accurately accounted for via ^{234}Th-based measurements is unclear, but we speculate that these small particles are in fact supplied to the mesopelagic by a process of slow, gravitational settling, representing a significant and underappreciated flux of organic material to the mesopelagic zone. Further we suggest that the inability to quantify this process could contribute to the deficit of measured carbon supply relative to metabolic carbon demand in mesopelagic fauna and thus affect the mesopelagic carbon budget observed at OSP (Nicholson *et al.*, in progress) and elsewhere (Burd et al. 2010).

Another implication of the finding that small particles form the base of the mesopelagic zooplankton food web is that the mesopelagic community is repackaging small, slowly settling particles into larger faster sinking fecal pellets, thus enhancing carbon flux in the mesopelagic. This repackaging is one possible explanation for the $\delta^{15}N_{SAA}$ values we observed in the 500 m sediment trap, which were elevated relative to the shallow traps. While this is an enticing concept, the net impact of repackaging on export processes remains unclear, and will depend in part on the efficiency with which material from small particles is converted into fecal material. Pairing the improved understanding of mesopelagic zooplankton trophic ecology afforded by this study with recent findings of Doherty et al. (2021) regarding fecal pellet production efficiency could help improve our understanding of this process and whether or not it represents a biogeochemically relevant process.

The ability to assess the food web base using CSIA-AA below 500 m was hampered by a lack of particle samples at deeper depths, however in zooplankton samples we observe even higher $\delta^{15}N_{SAA}$ into the deep mesopelagic which is most evident in the 0.2-0.5 and 1-2 mm zooplankton size classes (Figure 2a,b). If the $\delta^{15}N_{SAA}$ values of 1-6 μm particles stabilizes in the upper mesopelagic, as appears to occur at station ALOHA (Hannides et al. 2020) and in the equatorial Pacific (Romero-Romero et al. 2020), this could be an indication that the zooplankton food web incorporates material derived from even smaller particles through the lower mesopelagic and below.

4.2 Assessing the presence of bacterial biomass at the base of the food web

Synthesis of amino acids by heterotrophic bacteria generates biomass with a unique set of $\delta^{13}C_{EAA}$ values which can be identified using multivariate analyses (Larsen et al. 2009). This $\delta^{13}C_{EAA}$ "fingerprint," can then be traced into the zooplankton food web, such that the presence of bacterial biomass at the base of the food web can be recognized (Hannides et al. 2013). Since the increases in $\delta^{15}N_{SAA}$ values of particles with depth observed here (Figure 1) are generally attributed to extracellular enzymatic hydrolysis by particle associated microbes (Hannides et al. 2013; Ohkouchi et al. 2017), we hypothesized that bacterial biomass would make up some portion of the POM pool as degradation progressed, and thus contribute to zooplankton nutrition at depth.

Instead, when an LDA is used to assess the production end members contributing to the base of the zooplankton food web, we observe that the $\delta^{13}C_{EAA}$ fingerprint of zooplankton entirely overlaps with those of algae (Figure 5). Small excursions in LD1 and LD2 are observed with depth, and a significant trend in LD2 is observed when the deepest data point is omitted, but the effect size is small and at all depths the $\delta^{13}C_{EAA}$ fingerprints of zooplankton look primarily algal in character. These results are similar to those observed at Station ALOHA by Hannides et al. (2013), and oppose the idea that bacterial biomass is playing a significant role in the zooplankton food web. Here, however, it should be acknowledged that the bacteria used to train the LDA were grown in laboratory culture and may not account for the metabolic diversity present in natural settings. Further work in identifying a wild-type bacterial end member could help add confidence to this result. In addition, like metazoans, bacteria need not synthesize amino acids *de novo* if they are present in their diet in sufficient quantities. If this was the case at OSP, it is possible that bacterial production would not necessarily produce a fingerprint which is distinct from microalgae.

4.3 Zooplankton trophic ecology and the role of heterotrophic protists

Another goal of this project was to assess zooplankton food web structure and the role of heterotrophic protists as trophic intermediaries in the mesopelagic zone. Gutiérrez-Rodríguez et al. (2014) and Décima et al. (2017) have shown that, in laboratory cultures of *Oxyhris marina*, an estimate of trophic position based on the $\delta^{15}N$ values of alanine and phenylalanine is sensitive to protistan metabolism while one based on the $\delta^{15}N$ values of glutamic acid and phenylalanine is not. Therefore, by comparing $\mathrm{TP}_{\mathrm{ala–phe}}$ and $\mathrm{TP}_{\mathrm{glu–phe}}$ we were able to quantify the role of protistan heterotrophy throughout the water column. While our concept of phytoplankton production dynamics and zooplankton trophic ecology is well constrained within the euphotic zone at OSP (Goldblatt et al. 1999), making this determination in the mesopelagic represents a valuable contribution to our understanding of the mesopelagic food web at OSP.

Goldblatt et al. (1999) noted a transition below the mixed layer at OSP ($\sim$35 m) from a microalgal-based food web to one based on detritus. In our study, particle TP increased consistently with depth (Figure 3), indicating a shift with depth away from an algae-based food web, though particles do not appear to be predominantly detrital until $>$100 m. Doherty et al. (2021)

recently suggested that trophic position of fecal pellets can be elevated relative to phytodetritus because of colonization by microbes or because they contain remnants of heterotrophic biomass. Given that $\delta^{13}C_{EAA}$ fingerprint analysis of the zooplankton community based on those particles did not implicate bacterial biomass, we interpret this increase in TP as an increased contribution of fecal pellets to the POM pool with depth. In the case of small particles, these fecal pellets may be produced by extremely small taxa, or by disaggregation of larger fecal pellets in the upper mesopelagic.

For consumers, an accurate determination of trophic position should be made in reference to the base of the food web. In most systems this is implicit in amino acid based calculations of trophic position, as it is accounted for using the β parameter which is defined as the difference between the δ^{15}N values of trophic and source amino acids in primary producers. However, this is based on the assumption that primary producers form the base of the food web. Here, we see that the mesopelagic zooplankton food web is based mainly on in-situ particles smaller than 6 μm that are detrital in character. As a result, the difference between δ^{15}N in trophic and source amino acids in small particles is greater than in primary producers, which results in estimates of $\mathrm{TP} > 1$ in particles (Figure 7c). In order to make an accurate determination of zooplankton trophic position relative to small particles at depth, we simply subtracted the average 1-6 μm particle TP within each depth strata from the respective zooplankton TP, and add 1, to obtain $\mathrm{TP(in-situ)}$ (Figure 4a, Figure 7e), which is equivalent to redefining the β parameter in reference to in-situ particles. This may not be accurate for specific taxa which vertically migrate or feed on vertical migrators, but for the bulk of the community, whose food web base is dominated by in-situ small particles, this should be a reasonable assumption. Once this is accounted for, we can begin to draw conclusions about trophic structure in the zooplankton community.

In zooplankton throughout the water column, $\mathrm{TP_{ala-phe}}$ is consistently greater than $\mathrm{TP_{glu-phe}}$ (Figure 7a), with $\Delta\mathrm{TP_{ala-phe}} = 1.6$ on average, indicating that protists were actively involved in the food web at all depths. In 1-6 μm particles, however, $\mathrm{TP_{ala-phe}}$, $\mathrm{TP_{glu-phe}}$, and $\mathrm{TP_{tr-src}}$ were similar (Figure 7b), with $\Delta\mathrm{TP_{ala-glu}} = 0.3$ on average. As a result, values of $\Delta\mathrm{TP_{ala-phe}(in-situ)}$ in zooplankton remained elevated after being adjusted relative to in-situ small particles (Figure 4b, Figure 7f), precluding the possibility that this indication of protistan heterotrophy was inherited from detritus at the base of the food web. In the top 200 m, particle-adjusted

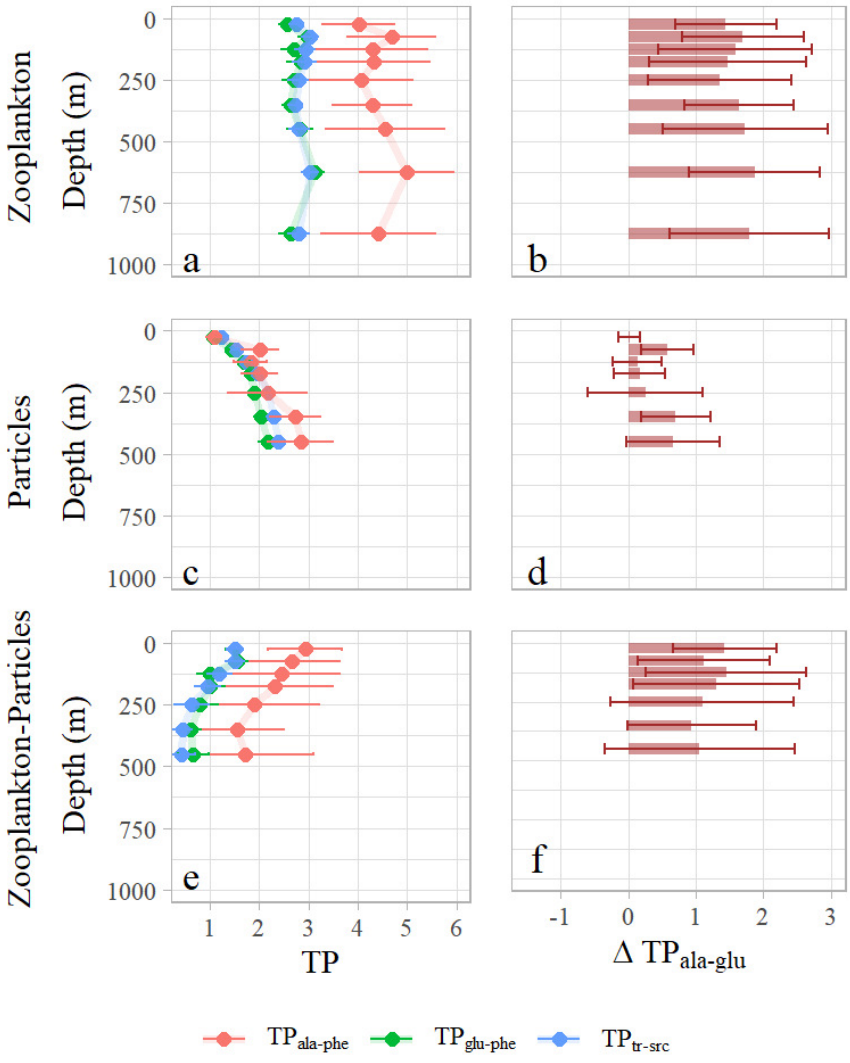

Figure 7: Comparison of average TP for all zooplankton and 1-6 µm particles plotted against depth. Panels **a**, **c**, and **e** show estimates of zooplankton and 1-6 µm particle trophic position where estimates of TP have been averaged by depth. Estimates of TP derived from different sets of source and trophic AAs are plotted where color differentiates the AAs used. Panels **b**, **d**, and **f** show the difference between $\mathrm{TP}_{\mathrm{ala-phe}}$ and $\mathrm{TP}_{\mathrm{glu-phe}}$ from the respective left hand panels.

$\Delta\mathrm{TP}_{\mathrm{ala–glu}}(\mathrm{in-situ})$ is consistently >1, suggesting that protists were responsible for *at least* one trophic step at these depths during the EXPORTS cruise to OSP. This finding is supported by the well documented paradigm that protistan microzooplankton are the major grazer of prokaryotic biomass, acting as a trophic link connecting the microalgal community to the mesozooplankton food web (Miller et al. 1991; Harrison et al. 1999). It also supports the recent finding of McNair and Menden-Deuer (2020) that active microzooplankton grazing occurs at the base of the euphotic zone. Moreover, the fact that particle-adjusted $\Delta\mathrm{TP}_{\mathrm{ala–glu}}(\mathrm{in-situ})$ remains elevated ($\Delta\mathrm{TP}_{\mathrm{ala–glu}}(\mathrm{in-situ}) = 1.0$ on average below 200 m) down to 500 m (Figure 4b) suggests that heterotrophic protists remain an active component of the community at least into the mid-mesopelagic zone, adding to to a body of relatively recent research using CSIA-AA to suggest that heterotrophic protists are ubiquitous in their role at the base of oligotrophic food webs (Landry and Décima 2017; Décima and Landry 2020; McNair and Menden-Deuer 2020; Landry et al. 2021; Bode et al. 2021).

Radiolaria (often >5 mm) were present in large quantities in some samples from the lower mesopelagic zone, and were isolated for $\delta^{15}\mathrm{N}_{\mathrm{SAA}}$ analysis. As a heterotrophic protist, we hypothesized that radiolaria would have a $\Delta\mathrm{TP}_{\mathrm{ala–glu}}$ higher than the background community and a comparatively low $\mathrm{TP}_{\mathrm{glu–phe}}$, but neither $\mathrm{TP}_{\mathrm{glu–phe}}$ nor $\Delta\mathrm{TP}_{\mathrm{ala–glu}}$ were substantially different from those of the nighttime zooplankton community collected at those depths. This indicated that nitrogen isotope fractionation of glutamic acid was occurring to a similar extent in radiolaria as in the metazoan community, suggesting that at least some wild protozoa do fractionate nitrogen in amino acids beyond just alanine. This is inconsistent with what was observed in laboratory grown dinoflagellate *Oxyrrhis marina* (Gutiérrez-Rodríguez et al. 2014; Décima et al. 2017), and emphasizes that care should be taken when applying the findings of these studies to more diverse members of paraphyletic group, protists. To our knowledge, this is the first time CSIA-AA has been used to analyze a wild protozoan.

We also see variation in trophic position within the mesozooplankton community, with larger zooplankton (<2 mm) tending to be about one TP higher than smaller zooplankton (0.2-2 mm) at all depths where the four size classes were measured (Figure 3a,b). This is true regardless of whether $\mathrm{TP}_{\mathrm{glu–phe}}$ or $\mathrm{TP}_{\mathrm{ala–phe}}$ is considered, and suggests multiple trophic levels were present within the mesozooplankton food web. We also observe that $\mathrm{TP}(\mathrm{in-situ})$ appears to decrease

consistently across the community with depth (Figure 4, Figure 7e) which suggests decreasing food web length, transitioning from a >4 trophic level zooplankton food web in the mixed layer, to ∼3 trophic level zooplankton food web in the mid mesopelagic. Because declines in $\mathrm{TP_{ala–phe}(in-situ)}$ with depth are similar across zooplankton sizes, this decrease in food web length is likely due to decreasing complexity in the microzooplankton food web, of which protozoans are a part. In addition, direct consumption of particles by some small mesozooplankton could contribute to this trend. Because food web length affects the efficiency with which a food web processes carbon, these findings could inform estimates of zooplankton community carbon demand, with specific implications for how we estimate community respiration across depth.

Three out of four chaetognath samples had trophic positions that were lower than would be expected if these taxa were feeding exclusively on resident mesopelagic zooplankton participating in an in-situ, particle-based food web (Figure 3c, d). *Metridia spp.* and small zooplankton collected in the mixed layer at night, however, had among the lowest unadjusted trophic positions in the community because their food web was based on fresh microalgae. If mesopelagic predators were feeding in part on diel vertical migrators like *Metridia spp.*, it could help explain their unexpectedly low trophic positions. In fact, $\mathrm{TP_{ala–phe}}$ for chaetognaths tended to be ∼1 trophic level higher than *Metridia spp.* and 0.2-2 mm zooplankton from the mixed layer, supporting the idea that mesopelagic predators were consuming diel vertical migrators at depth to some extent. This is consistent with our finding that chaetognaths are acquiring some portion of their nutrients from fresh surface production. In addition, we see that the one chaetognath sample with an elevated trophic position (2-5 mm size class from 300-400 m depth, Figure 3d) also had an elevated $\delta^{15}\mathrm{N_{SAA}}$ value (Figure 2d). This is consistent with the individuals in that sample predominantly relying on in-situ resources instead of preying on vertical migrators, suggesting that variation in resource acquisition strategies exists within the chaetognath community.

One challenge in interpreting these data is dealing with the high degree of uncertainty around $\mathrm{TP_{ala–phe}}$ (roughly twice that of $\mathrm{TP_{glu–phe}}$ or $\mathrm{TP_{tr–src}}$) and $\Delta\mathrm{TP_{ala–glu}}$, despite good accuracy in analytical determinations of δ^{15}N values for both ala and phe. This is mainly due to uncertainty in $\mathrm{TDF_{ala–phe}}$ and $\beta_{\mathrm{ala–phe}}$ which gets propagated through the trophic position calculation. This sometimes results in estimated uncertainty which is similar in magnitude to the features of ecological interest, hindering the ability to assign statistical significance to variations in $\mathrm{TP_{ala–phe}}$.

Yet, we see that at times both $\mathrm{TP_{glu–phe}}$ and $\mathrm{TP_{tr–src}}$ give unrealistically low estimates of trophic position (i.e., $\mathrm{TP_{glu–phe}(in-situ)} < 1$ for small zooplankton through much of the mesopelagic; Figure 4). Therefore, despite the large uncertainty, we consider $\mathrm{TP_{ala–phe}}$ to be a more accurate representation of zooplankton trophic ecology, though acknowledge that taking this approach reduces our precision around specific determinations of trophic position and food web length.

4.4 Implications for active transport as a source of carbon to the mesopelagic

Previous studies using $\delta^{15}\mathrm{N_{SAA}}$ values to assess the importance of small particles (defined as those <53 μm in previous studies) as a basal resource in the North Pacific have found that their importance can vary regionally and seasonally (Hannides et al. 2013, 2020; Gloeckler et al. 2018; Romero-Romero et al. 2020). Romero-Romero et al. (2020) synthesized these observations by hypothesizing that that when particle flux and migrator biomass is low, small particles are more likely to be an important basal resource to the mesopelagic zooplankton community. They found that the fractional contribution of small particles ($\mathrm{f_{small}}$) to the base of the food web was negatively related to both ^{234}Th flux at 200 m (suggested as a proxy for particle export) and the biomass of migratory zooplankton entering/exiting the mesopelagic zone each day/night, with the latter relationship proving to be statistically significant (Figure 8a,b).

Our results from OSP do not support the relationship between $\mathrm{f_{small}}$ and particle flux hypothesized in Romero-Romero et al. (2020) (Figure 8a). At OSP, ^{234}Th flux at 200 m (1028 ± 696 $\mathrm{dpmm^{-2}d^{-1}}$, Buesseler et al. (2020)) exceeded all of those reported in Romero-Romero et al. (2020) (Table 6), yet $\mathrm{f_{small}}$ was high for all zooplankton size classes (Table 3). Results from OSP do, however, support the reciprocal relationship between $\mathrm{f_{small}}$ and migrant biomass noted by Romero-Romero et al. (2020) (Figure 8b). Cruise average migrant biomass integrated from 200-1000 m at OSP was 258 mg $\mathrm{m^{-2}}$, which is similar to what was measured in the Equatorial Pacific at 5N and 8N (Table 6). These sites represent weak DVM end members compared to station ALOHA in the winter and summer and, like at OSP, the mesopelagic zooplankton food web appeared to be based primarily on small particles.

Oceanographic properties varied between OSP, station ALOHA, and the equatorial stations 5N and 8N. The summer mixed layer and euphotic zone are both substantially shallower at OSP

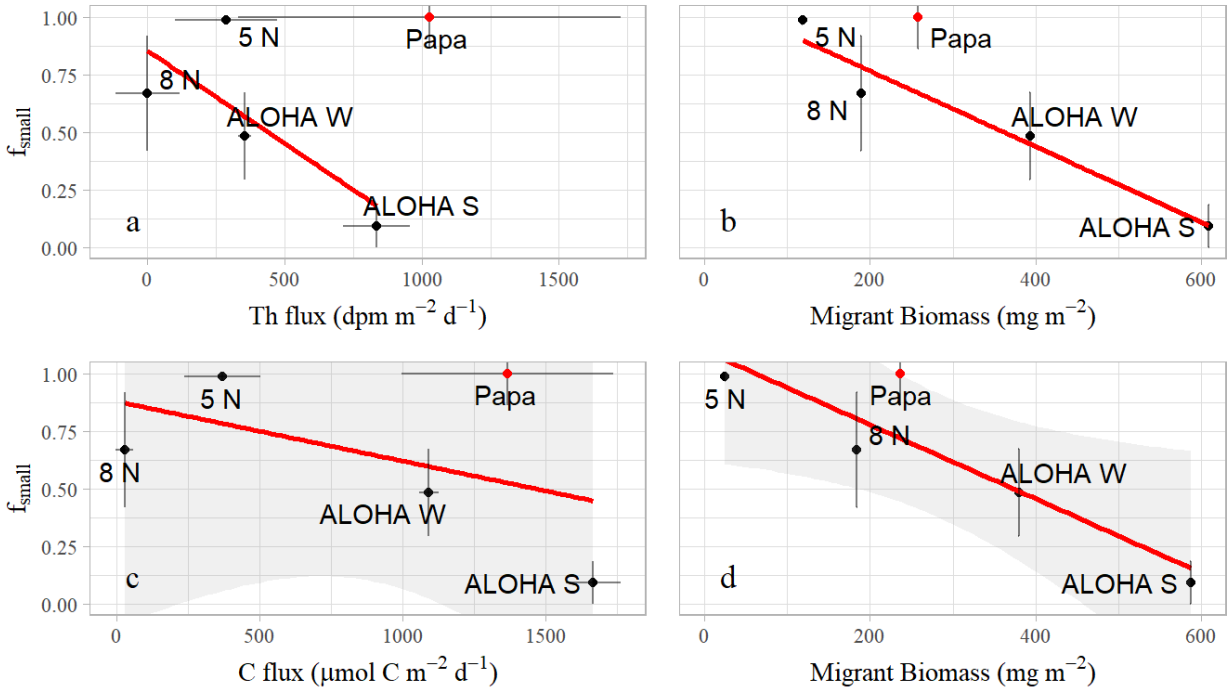

Figure 8: Relationships between f_{small} and (**a**) ^{234}Th flux at 200 m ($R^2 = 0.57$; ANOVA, $F_{1,2} = 2.60$, $p = 0.25$), (**b**) biomass of vertically migrating zooplankton integrated from 200-1000 m ($R^2 = 0.95$; ANOVA, $F_{1,2} = 35.86$, $p = 0.03$), (**c**) carbon export, estimated as the average C flux in the 100 m below the primary production zone (PPZ) ($R^2 = 0.22$, ANOVA, $F_{1,3} = 0.85$, $p = 0.42$) and (**d**) biomass of vertically migrating zooplankton integrated from below the PPZ to 1000 m ($R^2 = 0.81$, ANOVA, $F_{1,3} = 13.10$, $p = 0.04$). Data points are shown with uncertainty where applicable and regressions are shown in red, with the standard deviation about the regression highlighted in grey. Plots **a** and **b** reflect the relationships hypothesized in Romero-Romero et al. (2020), and so linear regressions and the related statistics do not include data from OSP. Regressions and statistics presented for Plots **c** and **d** include data from all sites.

Table 6: Parameters describing production and particle flux into the mesopelagic are tabulated along with the two-component $\delta^{15}N_{SAA}$ mixing model results (f_{small}) for 1-2 mm zooplankton. CbPM refers to estimates of NPP derived from the Carbon-based Productivity Model (Behrenfeld et al. 2005) and remotely sensed ocean color data.

	5 N	8 N	ALOHA W	ALOHA S	Papa
NPP ($\mathrm{mg\,C\,m^{-2}\,d^{-1}}$)	523 (CbPM)	323 (CbPM)	260 (^{14}C)	633 (^{14}C)	156 (^{14}C)
PPZ depth (m)	166	161	168	180	118
^{234}Th Flux at 200 m ($\mathrm{dpm\,m^{-2}\,d^{-1}}$)	287 ± 187	0 ± 117	355 ± 23	836 ± 121	1028 ± 696
C Export ($\mu\mathrm{mol\,C\,m^{-2}\,d^{-1}}$)	370±133	28±32	1092±34	1666±95	1367±369
Migrant Biomass (200 m, $\mathrm{mg\,m^{-2}}$)	118	189	393	609	258
Migrant Biomass (PPZ, $\mathrm{mg\,m^{-2}}$)	25	184	380	587	236
f_{small} (1-2 mm zoop.)	0.98±0.02	0.67±0.25	0.48±0.19	0.09±0.09	1±0.06

(Table 6), there was between site variation in the C:Th ratios of particles (Umhau et al. 2019; Buesseler et al. 2020), and also variation in NPP as determined by satellite ocean color and ^{14}C incubations (Table 6). The relative abundance of zooplankton size classes also varied between sites (Figure 6). Because these unique communities respond specifically to their local environment, between-site variation in both background properties and community structure can mask more general biogeochemical relationships, especially as the sites included in the comparison of Romero-Romero et al. (2020) become more diverse, spanning a greater breadth of oceanographic conditions. We attempted to control for some of this variation by adjusting the relationships presented in Romero-Romero et al. (2020) to account for euphotic zone depth and POM C:Th ratios.

Recent work by Buesseler et al. (2020) suggests that models which use fixed reference depths in the context of the biological carbon pump can misrepresent export efficiency and have deleterious effects on predictive models which extend across varied oceanographic provinces. In this case, the depth of the primary production zone (defined using in-situ fluorescence as in Owens et al. (2015)) ranged from 118 m at OSP to 180 m at Station ALOHA in the summer, and so carbon export and deep migrant biomass were redefined relative to the bottom of the primary production zone (PPZ) instead of 200 m (Table 6). Since C:Th affects the accuracy of ^{234}Th flux as a proxy for particle flux, we instead used ^{234}Th-derived carbon flux (Umhau et al. 2019; Buesseler et al. 2020) as a metric of particle supply to the mesopelagic. Additionally, a large degree of spatial heterogeneity in C flux was observed around the base of the PPZ at some sites and so C flux was averaged over 100 m immediately below the PPZ.

Romero-Romero et al. (2020) and previous studies (Hannides et al. 2013, 2020) used 1-2 mm zooplankton as a representative size class at 5N, 8N, and Station ALOHA because they were often the most abundant size class among those <5 mm. This excludes much of the carnivorous portion of the community that consume vertical migrators, which allows the *particulate* resources contributing to community metabolism in particular to be more accurately assessed. Therefore, while we feel that the biomass weighted average presented here is a more accurate representation of the resources utilized by the entire mesopelagic zooplankton community surveyed at OSP, we used $\mathrm{f_{small}}$ of 1-2 mm zooplankton to compare to previous studies.

By redefining the relationships suggested in Romero-Romero et al. (2020) using a more dynamic set of parameters (Table 6) and including our results we do not improve the relationship between small particle reliance in the mesopelagic and deep migrant biomass (Figure 8d; $\mathrm{R^2} = 0.81$; ANOVA, $\mathrm{F_{1,3}} = 13.105$, $\mathrm{p} = 0.04$), but do find that the relationship is still significant when OSP is included. Overall, this strengthens support for the hypothesis that small particles become a more important source of material to the mesopelagic food web when migrant biomass is low. The relationship between $\mathrm{f_{small}}$ and particle flux, however, deteriorated when results from OSP were included in the relationship proposed in Romero-Romero et al. (2020) as well as the new parameterization (Figure 8c; $\mathrm{R^2} = 0.22$; ANOVA, $\mathrm{F_{1,3}} = 0.84$, $\mathrm{p} = 0.43$). This suggests that carbon flux into the mesopelagic is not a primary control on zooplankton reliance on small particles.

Implicit in the mixing model results discussed above is the assumption that passively sinking particles (e.g. large or small particles) are the dominant vectors of material supply to the mesopelagic, yet the relationship we observe between $\mathrm{f_{small}}$ and migrant biomass emphasizes the role of DVM as a significant supply of material to the deep sea. Moreover, the tight reciprocal nature of this relationship suggests that, in fact, actively transported material could be the main alternative end member to small particles in these systems, instead of large particles. One possible mechanism is that fecal pellets produced by vertically migrating zooplankton at depth are incorporated into the mesopelagic food web. Because most 1-2 mm zooplankton are not large enough to consume vertical migrators directly, this is probably the process responsible for the trend observed in Figure 8b. Our analyses at OSP, however, only showed $\mathrm{f_{small}} < 1$ for the larger size classes. Taxonomic analyses of these size classes at OSP revealed that chaetognaths made up

a significant portion of the mesopelagic zooplankton community, particularly at night when they composed on average 33% of the 2-5 and >5 mm community abundance. Known to be ambush predators, chaetognaths are predominantly carnivorous and have been observed in captivity to prey on individuals about 1/10 their size (Saito and Kiørboe 2001). They are *not* expected to feed directly on large particles. Moreover, chaetognath $\delta^{15}N_{SAA}$ values and TP estimates indicate that some portion of their nutrition was from fresh surface production via consumption of vertically migrating zooplankton in the smaller size classes, and so we suggest that this is a more likely pathway for the incorporation of low-$\delta^{15}N_{SAA}$ material into the mesopelagic food web than direct consumption of large particles.

A similar $\delta^{15}N_{SAA}$ mass balance approach as was used to understand the importance of small particles can be used to understand chaetognath resource utilization. We assume that deep mesopelagic chaetognaths (2-5 and >5 mm individuals from 500-750 m, $\delta^{15}N_{SAA} = 2.8 \pm 0.2‰$) were eating some combination of vertically migrating zooplankton (defined as an average of 1-2 mm *Metridia spp.* collected at 0-50 m with $\delta^{15}N_{SAA} = 0.0 \pm 0.1‰$, and 1-2 mm *Neocalanus spp.* collected at 500-750 m with $\delta^{15}N_{SAA} = -0.5 \pm 0.2$) and small resident zooplankton (defined as 1-2 mm zooplankton collected at 500-750 m, $\delta^{15}N_{SAA} = 4.9 \pm 0.2‰$). If this was true, chaetognaths collected at 500-750 m would have to source about 40% of their amino acid nitrogen from vertically migrating animals. The same analysis carried out for chaetognaths collected at 300-400 m indicates 25% of their nitrogen came from vertical migrators. Although this does not represent the majority of their diet, because of their large numbers, this suggests that a significant amount of actively transported carbon likely passes through chaetognaths and is converted to biomass, fecal pellets, and dissolved inorganic carbon. Chaetognaths have been found to be important components of mid-water energy flow and flux production at other sites, and their feeding rates have been documented (Terazaki 1995; Kruse et al. 2010), but we are not aware of any instances where chaetognath respiration models have been used to specifically estimate energy flow through chaetognaths due to predation of vertical migrators. This could help to better understand the biogeochemical role of mid-water carnivorous taxa as it relates to active transport and the biological pump. In addition, vertical migrator mortality at depth has previously been a challenging quantity to estimate, though it is useful in estimating active transport of carbon to

depth. Estimating vertical migrator mortality due to chaetognath predation may provide a valuable constraint on current estimates of vertical migrator mortality in the mesopelagic.

Hannides et al. (2020) suggested that fresh surface material is an important resource for mid-water zooplankton communities at station ALOHA, and their isotope mass balance mixing mixing model implicated fast sinking particles as the vector for delivery to that food web. While at OSP we see only minor reliance on relatively fresh material, our results suggest that the small amount of fresh material that is utilized is incorporated into the zooplankton food web through carnivory of vertical migrators. This only became apparent when $>$2 mm zooplankton were considered. $>$2 mm zooplankton were abundant throughout the mesopelagic at the sites considered in Romero-Romero et al. (2020), making up 58-76% of the nighttime biomass collected between 200-1000 m (Figure 6). In addition, migrator biomass at Station ALOHA is roughly twice that observed at OSP (Figure 8c). This creates the potential for similar supply pathways driven by vertical migration and carnivory at depth at other sites which would not have been characterized in past studies of basal resources.

Considering the reciprocal relationship between migrator biomass and $\mathrm{f_{small}}$, we speculate that at sites where migrant biomass is high the mid-water zooplankton community is released from sole dependence on passive flux from small, detrital material. If this is true, then not only does vertical migration contribute to flux by actively transporting particles and potential prey items into the mesopelagic, but it could also modulate the degree to which the mesopelagic zooplankton community depends on gravitational flux, thus affecting their contribution to flux attenuation. All together this points to multiple mechanisms (i.e., in-situ supply of fecal pellets, supply of prey items, and release from dependence on gravitational flux) by which the strength of diel vertical migration could be affecting export pathways in the mesopelagic.

These results also highlight how the mode of material supply to the mesopelagic can vary both regionally and within a community, which is important to consider when interpreting mixing model results such as those presented here. For example, our mixing model assumes that in-situ materials are the only potential sources of material to the mesopelagic food web, and we see this assumption breakdown in our in-situ small/large particle based mixing model predictions for *Neocalanus spp.*. When individuals collected in the deep mesopelagic at night are used as the mixture, a small particle reliance of -0.53 ± 0.25 is returned. At the time of sampling, *Neocalanus spp.*

were believed to be entering diapause. Their mouth parts had atrophied and they had stockpiled nutrients from the surface as biomass before migrating to depth to reproduce (Mackas et al. 1998). As a result, in-situ particles are clearly not an appropriate representation the resources utilized by this taxa. This may be less obvious, however, for an animal that consumes these migrating copepods at depth (e.g., chaetognaths) and so we are more likely to mischaracterize their food web, which challenges our ability to use isotopic approaches alone to generate accurate inferences about their role in biogeochemical cycles. Further, it highlights the need for more sophisticated mixing models to be developed which can differentiate multiple sources of material the across depth. The identification of additional tracers (isotopic or not) will be key to such models' ability to resolve materials of unknown provenance and/or more accurately account for uncharacterized ecological variability within/between sites.

5 Conclusion

This study provides a detailed description of mesopelagic zooplankton food web structure at Ocean Station Papa (summarized in Figure 9) based on compound specific stable isotope analysis of amino acids (CSIA-AA) along with several other supporting data sets. Measurement of $\delta^{15}N_{SAA}$ values in particles and zooplankton provide strong evidence for a mesopelagic zooplankton food web that is based primarily on 1-6 μm particles. $\delta^{13}C_{EAA}$ fingerprinting analysis suggests that bacterial biomass is not likely contributing to zooplankton nutrition. Comparison of the $\delta^{15}N$ values of source and trophic amino acids provides an estimate of food web length which decreases significantly with depth, and also suggests protistan microzooplankton as a key component of the food web, occupying the lower trophic levels from the surface to at least 500 m. Finally, CSIA-AA of specific taxa helps quantify the impact of vertically migrating zooplankton on the diet of mesopelagic chaetognaths, and supports prior knowledge regarding ontogenetic and diel vertical migration in two copepod species. Together, these results emphasize the importance of small (<6 μm), slowly settling particles as a source of carbon to the mesopelagic in low productivity regions, and highlight a need to better understand carbon supply and demand dynamics of these smallest size classes of organic material.

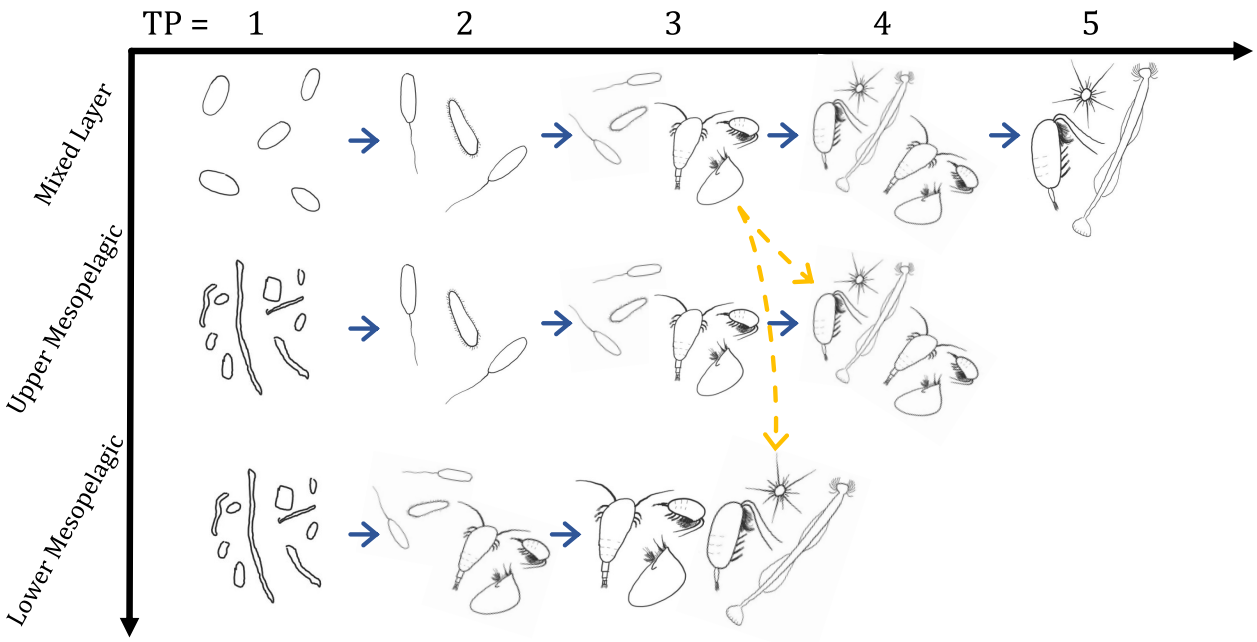

Figure 9: A schematic depicting a food web structure throughout the water column at OSP, with approximate trophic levels shown on the horizontal axis. Blue arrows indicate in-situ trophic transfer, while yellow arrows indicate carnivory of vertical migrators. Primary producers formed the base of the food web in the surface mixed layer and the zooplankton food web became increasingly detritus based with depth, becoming predominantly fecal in character within the upper mesopelagic. The zooplankton food web in the upper 100 m of the water column was fairly complex, with the micro and meso zooplankton food webs each containing more than one trophic level. In the mesopelagic, the food web base was largely composed of small particles ($<$6 μm), and while some of this material was sourced from surface waters via predation of vertical migrators, the large majority of it (72-96%) was sourced in-situ from the small particle pool. Particles entered the zooplankton food web through the microzooplankton community, and microzooplankton were in turn consumed by larger metazoans (mesozooplankton). Fod web length decreased into the mesopelagic, due in part to decreased complexity in the microzooplankton community, resulting in a $\sim$3 step food web by the mid mesopelagic zone. In addition to participating in the in-situ food web, predatory zooplankton such as chaetognaths and radiolaria were able to partially release themselves from total reliance on the deep, small particle based food web by consuming vertically migrating zooplankton at depth.

6 Data Availability

Zooplankton and particle CSIA-AA data are available in the supplemental table below. They have been submitted to the BCO-DMO online repository and will be available at:
https://www.bco-dmo.org/project/768320
Zooplankton biomass and taxonomy data, sediment trap flux data, ^{234}Th concentration data, and oceanographic data from OSP can all be found at:
https://doi.org/10.5067/SeaBASS/EXPORTS/DATA001
^{234}Th concentration data from the equatorial and subtropical pacific is presented in Umhau et al. (2019) and can be found at https://doi.org/10.1594/PANGAEA.911424 . Zooplankton data from Romero-Romero et al. (2020) can be found at:
https://www.bco-dmo.org/dataset/806471

7 Supplemental Data Tables

Table 7: δ^{15}N values of zooplankton collected in MOCNESS tows.

				δ^{15}N (‰)														SD (‰)													
Type	Event	Size	Depth	Ala	Gly	Thr	Ser	Val	Leu	Iso	Pro	Asx	Met	Glx	Phe	Tyr	Lys	Ala	Gly	Thr	Ser	Val	Leu	Ile	Pro	Asx	Met	Glx	Phe	Tyr	Lys
Zooplankton	Day	1-2 mm	875	21.83	8.02	-5.96	3.25	14.06	12.44	17.23	15.17	14.13	3.03	18.67	1.26	1.21	1.11	0.40	0.42	0.65	0.31	0.61	0.21	0.10	0.28	0.11	0.34	0.52	0.87	0.62	0.22
Zooplankton	Day	0.2-0.5 mm	625	19.51	6.89	-13.70	4.93	15.24	12.91	14.89	14.01	13.29	-1.82	18.49	2.26	0.74	0.41	0.59	0.15	1.13	1.31	0.53	0.11	0.22	0.15	0.13	nd	0.28	0.56	1.09	0.45
Zooplankton	Day	1-2 mm	625	19.32	5.15	-11.59	3.67	12.64	10.50	13.43	12.72	13.55	2.88	16.91	0.55	1.69	2.19	0.22	0.11	0.25	0.40	0.58	0.19	0.56	0.30	0.16	0.74	0.14	1.00	0.36	0.22
Zooplankton	Day	0.2-0.5 mm	450	19.46	4.61	-13.41	4.96	13.81	11.51	12.43	14.26	14.10	2.79	18.36	0.71	2.79	2.61	0.22	0.12	0.28	0.24	0.23	0.18	5.42	0.24	0.28	0.75	0.37	0.39	0.93	0.70
Zooplankton	Day	1-2 mm	450	20.39	6.06	-13.25	4.13	13.63	10.91	13.18	12.36	13.59	4.04	17.60	1.05	2.64	2.77	0.72	0.17	0.28	0.69	0.38	0.21	0.57	0.16	0.12	0.77	0.20	0.64	0.77	0.52
Zooplankton	Day	0.2-0.5 mm	350	18.12	3.48	-14.98	4.72	13.54	11.38	13.86	12.22	13.23	2.72	18.16	3.95	1.29	2.69	0.15	0.18	0.75	0.44	0.14	0.25	0.33	0.05	0.20	0.42	0.11	1.02	0.13	0.55
Zooplankton	Day	1-2 mm	350	18.04	3.65	-9.44	2.92	12.22	8.99	10.94	10.66	12.87	3.50	16.42	0.14	3.84	2.77	0.24	0.06	0.27	0.18	0.22	0.29	0.30	0.26	0.18	0.83	0.14	0.80	0.75	0.11
Zooplankton	Day	0.2-0.5 mm	250	17.89	4.85	-10.04	5.66	14.71	12.06	15.49	13.12	12.98	2.20	18.25	-0.54	4.00	1.37	0.29	0.24	0.47	0.20	0.21	0.04	0.34	0.12	0.07	0.43	0.31	0.37	0.45	0.43
Zooplankton	Day	1-2 mm	250	18.87	3.62	-10.91	4.71	11.62	9.49	12.89	10.66	12.32	3.16	15.81	0.37	0.71	2.72	0.18	0.13	0.56	0.75	0.46	0.29	0.18	0.13	0.26	1.05	0.21	0.63	0.53	0.11
Zooplankton	Day	0.2-0.5 mm	175	17.32	4.74	-10.33	5.03	13.44	10.89	13.73	12.35	12.01	2.05	16.36	-1.28	1.79	1.45	0.38	0.05	0.68	0.42	0.61	0.17	0.34	0.27	0.19	0.89	0.20	0.27	0.64	0.28
Zooplankton	Day	1-2 mm	175	18.22	2.36	-14.02	4.95	12.14	9.40	12.73	10.50	12.15	5.00	16.16	4.59	0.05	2.63	0.06	0.15	0.41	0.29	0.29	0.18	0.31	0.22	0.17	0.39	0.13	0.65	0.86	0.05
Zooplankton	Day	0.2-0.5 mm	125	17.56	3.69	-15.62	5.07	14.33	11.01	12.80	12.24	11.97	3.14	16.54	1.04	2.40	2.87	0.27	0.18	0.49	0.19	0.07	0.15	0.06	0.27	0.33	1.23	0.08	0.41	0.88	0.34
Zooplankton	Day	1-2 mm	125	17.99	5.40	-15.43	7.55	13.56	11.01	13.53	10.51	12.34	2.85	15.35	-1.25	1.50	1.81	0.40	0.23	0.31	0.28	0.43	0.34	0.52	0.21	0.24	0.93	0.29	0.89	0.31	0.56
Zooplankton	Day	0.2-0.5 mm	75	14.39	0.93	-17.95	1.42	13.30	11.36	12.73	10.27	9.11	1.94	14.15	-0.69	1.49	1.72	0.24	0.21	0.50	0.11	0.13	0.35	0.77	0.18	0.17	0.57	0.07	0.09	0.01	0.36
Zooplankton	Day	1-2 mm	75	14.88	1.98	-6.99	2.59	9.84	6.26	9.43	7.07	9.08	0.38	11.76	2.46	-3.78	-1.75	0.38	0.21	0.68	1.07	0.93	0.13	0.18	0.36	0.31	0.49	0.18	0.89	0.33	0.18
Zooplankton	Day	0.2-0.5 mm	25	12.32	-0.13	-2.30	-0.64	7.97	7.89	9.36	8.89	8.33	-2.03	11.01	1.69	2.92	1.80	0.34	0.42	0.76	0.05	0.58	0.17	0.66	0.10	0.05	nd	0.59	0.78	0.39	0.12
Zooplankton	Day	1-2 mm	25	16.45	0.82	-8.42	0.20	10.08	8.86	11.10	10.68	11.43	2.03	14.29	1.11	0.76	-1.18	0.04	0.25	0.31	0.85	0.71	0.19	0.31	0.51	0.09	0.19	0.01	0.91	0.61	0.28
Zooplankton	Night	0.2-0.5 mm	875	22.40	10.60	-10.30	8.10	2.10	15.50	19.30	15.60	14.30	nd	18.20	3.80	5.00	2.50	0.55	0.41	0.81	0.80	0.30	0.27	0.65	0.64	0.60	nd	0.52	0.96	0.23	0.16
Zooplankton	Night	1-2 mm	875	22.50	8.60	-15.30	8.70	13.90	15.10	16.80	15.70	15.30	nd	19.50	3.90	6.30	2.30	0.59	0.10	0.34	0.25	0.37	0.70	0.40	0.21	0.36	nd	0.31	0.72	0.50	0.51
Zooplankton	Night	0.2-0.5 mm	625	20.50	8.40	-13.50	7.70	9.40	14.20	17.70	15.50	14.20	nd	19.30	0.90	3.90	3.40	0.53	0.34	0.67	0.65	0.62	0.36	0.61	0.72	0.39	nd	0.46	0.41	0.43	0.41
Zooplankton	Night	1-2 mm	625	23.00	7.80	-12.20	7.80	11.50	14.40	15.20	14.20	13.70	nd	18.10	2.20	5.20	1.70	0.17	0.07	0.33	0.44	0.84	0.27	0.68	0.42	0.13	nd	0.15	0.50	0.49	0.13
Zooplankton	Night	2-5 mm	625	23.02	7.49	-13.27	7.01	15.95	14.49	16.95	15.57	16.21	4.61	20.35	0.17	3.79	2.47	0.34	0.33	0.26	0.40	1.03	0.14	0.19	0.20	0.14	0.93	0.28	1.50	0.72	0.20
Zooplankton	Night	5 mm	625	20.63	5.81	-12.97	5.94	15.12	15.13	16.36	15.00	14.73	4.37	18.42	-0.73	1.56	1.63	0.34	0.12	0.37	0.73	0.15	0.17	0.68	0.39	0.09	0.35	0.12	0.26	0.52	0.32
Zooplankton	Night	0.2-0.5 mm	450	18.73	5.85	-16.19	6.43	15.04	11.68	15.59	15.04	14.10	4.37	18.28	-0.61	2.99	2.13	0.79	0.33	0.38	0.56	0.42	0.16	0.79	0.10	0.49	nd	0.49	0.73	0.35	0.16
Zooplankton	Night	1-2 mm	450	22.40	7.00	-12.10	7.40	11.40	12.50	12.50	13.00	13.50	nd	17.20	3.30	4.90	1.40	0.25	0.30	0.99	0.28	0.58	0.27	0.39	0.15	0.19	nd	0.11	0.64	0.36	0.25
Zooplankton	Night	0.2-0.5 mm	350	19.80	6.50	-13.40	5.20	11.80	11.50	15.10	13.80	12.70	nd	17.70	4.70	2.70	1.10	0.49	0.22	0.26	0.18	0.13	0.11	0.32	0.19	0.14	nd	0.29	0.22	0.78	0.29
Zooplankton	Night	1-2 mm	350	20.90	6.10	-11.00	7.00	11.10	10.80	11.40	11.90	13.10	nd	16.80	3.90	5.60	2.60	0.26	0.24	0.67	0.23	0.59	0.17	0.57	0.33	0.13	nd	0.30	0.55	0.31	0.49
Zooplankton	Night	2-5 mm	350	19.54	5.09	-11.18	5.13	15.19	11.07	13.01	11.80	13.37	3.14	16.86	-1.18	4.92	1.94	0.26	0.18	0.77	0.69	1.07	0.16	0.43	0.24	0.05	0.92	0.07	0.68	0.53	0.30
Zooplankton	Night	5 mm	350	20.30	5.70	-16.51	5.76	16.23	15.10	15.23	12.83	14.36	nd	17.50	1.03	4.59	2.81	0.13	0.23	0.20	0.46	0.05	0.16	0.43	0.06	0.04	nd	0.14	0.34	0.46	0.23
Zooplankton	Night	0.2-0.5 mm	250	19.00	5.00	-16.10	6.20	13.80	11.80	15.00	13.30	12.70	nd	18.20	3.10	2.70	0.30	0.38	0.23	0.58	0.42	0.44	0.23	0.32	0.22	0.09	nd	0.17	0.43	0.66	0.43
Zooplankton	Night	1-2 mm	250	19.70	6.30	-16.60	7.50	13.20	12.60	13.40	12.10	13.30	nd	17.60	1.60	5.10	1.50	0.26	0.19	0.65	0.34	0.42	0.25	0.35	0.20	0.11	nd	0.35	0.68	0.53	0.52
Zooplankton	Night	0.2-0.5 mm	175	18.58	4.97	-15.53	2.55	13.17	13.25	16.09	14.72	13.54	nd	17.60	0.03	1.74	0.38	0.86	0.24	0.98	0.65	0.57	0.30	1.17	0.50	0.37	nd	0.77	1.54	0.69	0.24
Zooplankton	Night	1-2 mm	175	19.60	5.20	-16.50	6.70	13.60	12.60	13.20	12.50	13.00	nd	17.30	1.90	4.20	0.70	0.38	0.14	0.16	0.78	0.33	0.29	0.22	0.11	0.16	nd	0.11	0.81	0.80	0.28
Zooplankton	Night	0.2-0.5 mm	125	20.72	4.69	-14.85	-1.36	12.58	12.57	17.56	15.22	14.39	nd	17.99	2.33	3.35	0.31	0.13	0.03	0.79	0.54	0.22	0.38	0.80	0.25	0.14	nd	0.78	0.79	0.59	0.14
Zooplankton	Night	1-2 mm	125	19.20	1.90	-16.20	4.60	10.60	10.80	11.20	11.40	12.20	nd	16.90	1.60	4.40	0.90	0.35	0.10	0.38	0.39	0.69	0.25	0.29	0.33	0.07	nd	0.09	0.57	0.73	0.06
Zooplankton	Night	0.2-0.5 mm	75	17.03	1.01	-14.62	2.24	-1.72	9.37	7.82	10.72	10.14	nd	14.47	-3.63	-1.35	-0.53	0.92	1.07	1.32	0.28	1.54	1.31	2.74	0.89	0.27	nd	0.16	0.45	0.92	0.47
Zooplankton	Night	1-2 mm	75	16.70	0.80	-15.00	2.40	11.50	8.90	11.40	9.90	10.90	nd	16.10	1.10	0.90	-3.00	0.13	0.14	0.15	0.31	0.12	0.23	0.30	0.02	0.21	nd	0.08	0.10	0.60	0.09
Zooplankton	Night	2-5 mm	75	18.70	0.15	-13.75	3.96	12.61	10.50	11.48	10.74	12.21	2.32	15.80	-1.10	2.95	1.09	0.23	0.17	0.45	0.15	0.95	0.11	0.47	0.29	0.19	0.46	0.11	0.15	0.28	0.61
Zooplankton	Night	5 mm	75	20.04	1.37	-15.65	2.78	14.92	13.41	13.34	11.92	13.84	2.07	17.02	-3.04	3.08	3.02	0.18	0.23	0.52	0.03	0.57	0.16	0.20	0.09	0.08	0.09	0.04	0.26	0.36	0.28
Zooplankton	Night	0.2-0.5 mm	25	17.66	3.05	-12.03	2.84	9.09	10.97	13.49	11.38	10.69	nd	14.04	2.79	2.39	0.37	0.48	0.04	0.43	0.82	0.38	0.25	0.92	0.30	0.22	nd	0.30	1.48	0.54	0.15
Zooplankton	Night	1-2 mm	25	17.70	3.10	-12.50	4.00	10.40	10.50	11.10	10.00	10.90	nd	14.80	1.10	4.00	-0.40	0.48	0.18	0.61	0.22	0.98	0.18	0.11	0.55	0.10	nd	0.17	0.54	0.92	0.37
Zooplankton	Night	2-5 mm	25	15.63	0.87	-11.90	4.75	8.58	8.78	10.79	8.86	10.26	1.19	13.68	-0.84	3.09	0.82	0.11	0.39	0.68	0.17	0.20	0.23	0.39	0.16	0.14	0.94	0.08	0.39	0.12	0.38
Zooplankton	Night	5 mm	25	17.20	0.46	-14.65	1.98	14.50	11.13	13.09	9.11	11.73	3.59	16.76	-2.02	2.31	0.85	0.29	0.14	0.11	0.14	0.14	0.18	0.36	0.09	0.14	0.50	0.07	0.53	0.56	0.25
Metridia	Night	1-2 mm	25	12.95	-1.59	-12.39	3.15	10.74	6.42	9.28	7.23	9.74	4.53	13.32	-0.79	0.09	-0.95	0.39	0.12	0.6	0.14	0.37	0.12	0.47	0.14	0.21	0.73	0.11	0.32	nd	0.13
Neocalanus	Night	1-2 mm	625	14.82	1.11	-11.63	2.96	9.66	5.78	9.03	6.96	10.33	nd	13.34	-3.84	nd	-2.36	0.23	0.34	0.06	0.43	0.25	0.22	0.22	0.09	0.11	nd	0.17	0.45	nd	0.19
Chaetognath	Night	2-5 mm	625	18.27	3.41	-14.23	8.98	14.81	14.06	16.87	11.4	14.21	nd	17.76	-0.52	nd	0.38	0.34	0.84	0.53	0.06	4.05	0.36	0.95	0.71	0.09	nd	0.41	0.97	nd	0.78
Chaetognath	Night	5 mm	625	17.8	3.48	-13.7	8.44	16.56	13.2	16.19	10.96	12.79	nd	16.34	-0.66	nd	-1.23	0.65	0.69	0.74	0.52	0.34	0.15	0.56	0.09	0.26	nd	0.23	0.58	nd	0.44
Chaetognath	Night	2-5 mm	350	18.35	7.51	-14.37	6.58	15.35	13.51	16.74	11.5	12.92	3.8	17.48	0.58	nd	1.75	0.41	0.3	0.33	0.67	0.72	0.65	1.02	0.33	0.93	0.87	0.9	0.42	nd	0.8
Chaetognath	Night	5 mm	350	22.81	2.73	-17.9	6.33	22.7	18.75	20.16	13.62	15.57	4.28	20.59	0.85	nd	1.91	0.16	0.19	0.5	0.06	0.42	0.18	0.21	0.16	0.08	0.75	0.01	0.46	nd	0.39
Radiolarian	Day	5 mm	625	21.24	6.52	-13.34	5.07	16.58	14.52	16.32	14.07	15.2	4.25	18.12	1.16	5.17	0.97	0.14	0.15	0.68	0.19	0.63	0.38	0.44	0.43	0.17	0.88	0.11	0.6	0.2	0.23
Radiolarian	Night	5 mm	625	19.77	6.26	-12.48	7.9	19.18	15.44	16.66	14.06	14.06	4.81	17.71	0.12	3.87	-0.97	1.5	1.4	2.2	1.27	1.55	0.27	0.76	0.45	0.42	0.78	0.29	0.21	0.3	0.43

Table 8: δ^{13}C values of zooplankton collected in MOCNESS tows.

				δ^{13}C (‰)														SD (‰)												
Type	Event	Size	Depth	Ala	Gly	Thr	Ser	Val	Leu	Iso	Pro	Asx	Met	Glx	Phe	Tyr	Lys	Ala	Gly	Thr	Ser	Val	Leu	Ile	Pro	Asx	Met	Glx	Phe	Tyr	Lys
Zooplankton	Day	1-2 mm	875	-18.93	-12.73	-15.99	-5.23	-25.93	-29.92	-21.95	-18.44	-15.93	-21.43	-15.66	-23.65	-22.98	-20.66	0.32	0.61	0.54	1.11	0.50	0.25	0.41	0.15	0.27	0.41	0.29	0.75	1.37	0.86
Zooplankton	Day	0.2-0.5 mm	625	-21.85	-8.66	-15.68	-7.69	-29.17	-31.93	-23.47	-22.68	-17.76	-24.04	-19.59	-29.01	-26.47	-23.32	0.34	0.16	0.38	0.33	0.32	0.21	0.32	0.09	0.21	0.86	0.52	0.42	0.72	0.28
Zooplankton	Day	1-2 mm	625	-17.75	-14.75	-16.22	-6.08	-27.00	-30.27	-23.39	-18.07	-17.84	-23.38	-18.01	-24.15	-22.74	-19.63	0.40	0.77	2.12	1.79	0.64	0.56	0.87	0.82	0.44	1.05	0.45	0.39	1.50	1.21
Zooplankton	Day	0.2-0.5 mm	450	-20.41	-12.53	-14.36	-2.60	-26.34	-29.32	-20.91	-18.72	-15.89	-23.30	-16.82	-25.34	-25.48	-20.54	0.24	0.31	0.54	0.21	0.42	0.09	0.16	0.34	0.35	0.23	0.44	0.34	0.61	0.81
Zooplankton	Day	1-2 mm	450	-18.93	-16.48	-13.24	-5.99	-26.34	-30.17	-23.31	-17.94	-16.40	-20.87	-16.49	-22.66	-21.91	-21.60	0.30	0.30	0.49	1.59	0.24	0.18	0.32	0.75	0.49	0.34	0.30	0.29	1.27	0.76
Zooplankton	Day	0.2-0.5 mm	350	-19.97	-11.32	-16.29	-4.08	-27.46	-30.99	-22.15	-20.24	-15.66	-23.09	-17.51	-25.98	-24.81	-23.54	0.37	0.48	1.01	0.35	0.13	0.28	0.64	0.18	0.51	0.20	0.16	0.45	1.66	0.25
Zooplankton	Day	1-2 mm	350	-21.54	-13.02	-16.34	-9.98	-29.01	-32.36	-23.49	-21.81	-19.85	-25.43	-19.97	-29.84	-28.44	-22.54	0.86	0.80	0.50	0.38	0.39	0.30	0.62	0.11	0.39	0.81	0.39	0.14	0.49	0.38
Zooplankton	Day	0.2-0.5 mm	250	-21.13	-11.83	-15.26	-7.25	-28.81	-31.19	-23.34	-20.71	-18.66	-26.08	-19.43	-27.30	-24.18	-20.60	0.11	0.43	0.79	0.23	0.53	0.12	0.13	0.13	0.52	0.35	0.13	0.43	1.66	0.62
Zooplankton	Day	1-2 mm	250	-19.19	-15.63	-16.83	-5.61	-27.76	-31.02	-23.72	-18.61	-17.55	-24.15	-17.06	-24.40	-23.82	-21.45	0.51	0.29	0.28	0.63	0.75	0.19	0.37	0.30	0.22	0.53	0.26	0.39	0.67	0.14
Zooplankton	Day	0.2-0.5 mm	175	-21.04	-12.30	-16.17	-8.62	-29.19	-31.05	-23.46	-20.90	-19.36	-25.67	-19.20	-26.68	-24.02	-20.70	0.18	0.36	0.60	0.65	0.20	0.10	0.11	0.20	0.46	0.19	0.59	0.19	1.87	0.98
Zooplankton	Day	1-2 mm	175	-18.87	-15.41	-16.93	-5.22	-27.94	-31.11	-23.75	-18.50	-17.69	-22.95	-16.93	-24.30	-22.45	-20.68	0.24	0.74	1.06	0.91	0.19	0.12	0.18	0.83	0.47	0.67	0.50	0.40	1.19	0.28
Zooplankton	Day	0.2-0.5 mm	125	-23.09	-14.15	-17.49	-11.40	-31.49	-32.80	-23.93	-22.66	-21.44	-25.69	-20.55	-29.12	-27.11	-23.28	0.32	0.21	0.35	0.54	0.21	0.10	0.09	0.08	0.26	0.57	0.15	0.27	0.67	0.21
Zooplankton	Day	1-2 mm	125	-21.66	-9.65	-18.15	-9.10	-29.71	-31.72	-24.10	-21.19	-19.79	-24.08	-18.37	-28.55	-27.31	-22.57	0.37	0.38	0.48	0.21	0.25	0.03	0.28	0.60	0.09	0.62	0.12	0.14	0.24	1.25
Zooplankton	Day	0.2-0.5 mm	75	-22.15	-12.38	-16.43	-9.69	-30.04	-33.48	-23.09	-22.37	-19.23	-26.92	-20.24	-28.94	-27.32	-22.33	0.76	0.47	0.72	0.44	0.26	1.18	0.50	0.39	0.40	0.99	0.87	0.30	0.88	0.15
Zooplankton	Day	1-2 mm	75	-17.76	-13.54	-17.46	-8.61	-26.87	-30.55	-22.32	-19.36	-15.70	-20.98	-15.89	-23.67	-24.27	-20.63	0.17	0.10	0.72	0.90	0.31	0.20	0.50	0.19	0.11	0.50	0.32	0.57	0.56	0.65
Zooplankton	Day	0.2-0.5 mm	25	-21.24	-13.04	-17.28	-8.98	-28.78	-33.30	-23.63	-22.86	-19.30	-25.37	-20.26	-29.62	-26.75	-23.36	0.66	0.79	0.34	1.41	0.90	0.12	0.67	0.23	0.40	0.86	0.19	0.66	0.33	1.03
Zooplankton	Day	1-2 mm	25	-19.16	-9.89	-15.62	-8.40	-29.15	-33.78	-21.30	-21.26	-18.56	-24.01	-18.54	-27.67	-26.62	-22.14	0.33	0.37	0.45	0.88	0.09	0.83	0.66	0.09	0.32	0.41	0.69	0.35	0.20	0.43
Zooplankton	Night	0.2-0.5 mm	875	-19.50	-9.50	-13.40	-5.90	-25.40	-29.90	-20.10	-19.20	-15.50	nd	-16.50	-26.40	-24.80	-21.40	0.23	0.21	0.32	0.32	0.42	0.17	0.50	0.07	0.29	nd	0.19	0.95	0.59	0.38
Zooplankton	Night	1-2 mm	875	-17.90	-8.90	-11.70	-5.90	-25.70	-29.90	-20.60	-19.20	-16.50	nd	-16.40	-27.10	-25.70	-21.60	0.60	0.49	0.78	0.52	0.96	0.21	0.17	0.37	0.26	nd	0.23	0.36	0.41	0.28
Zooplankton	Night	0.2-0.5 mm	625	-18.80	-9.00	-11.90	-3.90	-26.10	-29.30	-20.60	-19.40	-14.80	nd	-15.70	-27.00	-26.50	-22.00	0.26	0.47	0.77	0.09	0.43	0.17	0.72	0.31	0.18	nd	0.21	0.78	0.09	0.12
Zooplankton	Night	1-2 mm	625	-19.30	-11.00	-12.10	-4.60	-27.60	-30.70	-21.40	-20.80	-19.50	nd	-19.10	-26.80	-25.70	-21.30	0.44	0.96	0.33	0.28	0.70	0.28	0.83	0.16	0.18	nd	0.13	0.29	0.43	0.24
Zooplankton	Night	2-5 mm	625	-21.30	-12.62	-15.54	-6.70	-28.46	-31.06	-22.69	-20.84	-19.98	nd	-20.18	-27.02	-27.69	-22.88	0.11	0.45	0.17	0.30	0.28	0.25	0.43	0.20	0.09	nd	0.15	0.71	0.10	nd
Zooplankton	Night	5 mm	625	-21.22	-10.85	-16.02	-5.07	-28.46	-30.77	-22.27	-19.26	-17.03	nd	-17.85	-26.44	-25.86	-21.46	0.18	0.11	0.66	0.21	0.50	0.07	0.36	0.20	0.06	nd	0.36	0.25	0.43	0.22
Zooplankton	Night	0.2-0.5 mm	450	-18.42	-7.60	-9.94	-0.92	-26.65	-29.90	-21.84	-18.05	-13.65	nd	-14.51	-26.49	-25.04	-21.68	0.29	0.48	0.69	0.68	0.32	0.29	0.22	0.12	0.62	nd	0.29	0.35	0.51	1.16
Zooplankton	Night	1-2 mm	450	-20.10	-11.00	-13.20	-6.50	-29.60	-31.30	-22.10	-20.10	-18.80	nd	-19.60	-26.70	-25.30	-21.20	0.56	0.60	0.68	0.59	0.02	0.47	0.09	0.24	0.31	nd	0.17	0.65	0.34	0.24
Zooplankton	Night	0.2-0.5 mm	350	-21.10	-14.00	-14.30	-6.50	-29.20	-31.60	-22.80	-20.60	-20.20	nd	-19.00	-25.70	-26.60	-22.90	0.75	0.62	0.07	0.58	0.52	0.02	0.66	0.02	0.24	nd	0.13	1.21	0.33	0.24
Zooplankton	Night	1-2 mm	350	-19.00	-9.90	-12.20	-6.90	-27.80	-31.30	-22.20	-21.10	-17.80	nd	-17.10	-27.50	-25.50	-20.80	0.26	0.49	0.73	0.34	0.16	0.21	0.45	0.10	0.17	nd	0.35	0.27	0.60	0.33
Zooplankton	Night	2-5 mm	350	-21.35	-11.79	-15.76	-6.49	-29.24	-31.90	-22.92	-21.35	-20.61	nd	-20.57	-28.02	-26.12	-22.01	0.16	0.04	0.30	0.66	0.47	0.10	0.14	0.30	0.18	nd	0.08	0.09	0.52	0.19
Zooplankton	Night	5 mm	350	-20.88	-9.63	-17.62	-3.62	-29.28	-31.33	-22.81	-20.19	-18.55	nd	-18.55	-27.61	-24.23	-21.24	0.26	0.41	0.22	0.82	0.21	0.13	0.20	0.16	0.45	nd	0.26	0.19	0.56	0.47
Zooplankton	Night	0.2-0.5 mm	250	-21.60	-12.30	-15.20	-9.10	-29.90	-31.30	-22.80	-20.70	-19.90	nd	-18.90	-28.00	-26.70	-22.80	0.45	0.89	0.42	0.96	0.22	0.30	0.67	0.07	0.69	nd	0.27	0.45	0.10	0.32
Zooplankton	Night	1-2 mm	250	-20.90	-12.40	-14.70	-2.40	-28.50	-30.90	-22.20	-19.90	-18.30	nd	-17.90	-27.50	-26.40	-18.70	0.56	0.76	0.45	0.34	0.89	0.17	0.12	0.72	0.36	nd	0.33	0.68	0.55	0.38
Zooplankton	Night	0.2-0.5 mm	175	-17.18	-7.54	-7.22	2.32	-25.22	-29.74	-20.70	-17.38	-13.10	nd	-13.48	-26.76	-26.35	-20.23	0.52	0.84	0.57	0.75	0.33	0.35	0.06	0.09	0.26	nd	0.46	0.34	1.03	0.27
Zooplankton	Night	1-2 mm	175	-21.20	-10.00	-14.00	-6.20	-29.50	-31.50	-22.60	-20.30	-19.50	nd	-19.70	-28.00	-25.30	-22.20	0.11	0.43	0.91	0.17	0.31	0.12	0.19	0.20	0.26	nd	0.09	0.29	0.42	0.22
Zooplankton	Night	0.2-0.5 mm	125	-17.33	-7.31	-7.86	2.91	-25.94	-29.84	-20.71	-17.62	-13.54	nd	-14.50	-26.92	-26.73	-21.43	0.23	0.58	0.11	1.07	0.05	0.27	0.33	0.26	0.65	nd	0.41	0.50	1.30	0.95
Zooplankton	Night	1-2 mm	125	-20.30	-12.30	-15.80	-5.10	-28.70	-31.10	-21.50	-19.70	-18.40	nd	-18.00	-27.30	-27.10	-18.30	0.44	0.38	0.52	0.42	0.57	0.15	0.12	0.25	0.30	nd	0.31	0.50	0.93	0.46
Zooplankton	Night	0.2-0.5 mm	75	-17.21	-6.14	-7.46	-0.10	-23.04	-29.54	-21.16	-17.54	-12.33	nd	-12.45	-26.36	-25.72	-19.73	0.30	0.68	0.43	0.72	0.30	0.37	0.26	0.26	0.36	nd	0.19	0.35	0.51	0.98
Zooplankton	Night	1-2 mm	75	-18.10	-8.40	-12.20	-5.50	-26.50	-30.30	-20.00	-19.30	-16.20	nd	-15.70	-26.40	-25.70	-20.80	0.15	0.11	0.53	0.56	0.12	0.27	0.61	0.14	0.23	nd	0.32	0.41	0.37	0.37
Zooplankton	Night	2-5 mm	75	-20.02	-12.17	-15.62	-7.87	-30.94	-32.18	-23.20	-19.91	-18.52	nd	-16.79	-27.67	-26.87	-20.79	0.27	0.40	0.28	0.35	1.74	0.64	0.34	0.13	0.41	nd	0.27	0.62	0.24	0.17
Zooplankton	Night	5 mm	75	-19.95	-6.19	-13.05	-4.82	-29.83	-31.24	-22.87	-20.36	-19.09	nd	-19.69	-28.78	-26.75	-21.51	0.34	0.39	0.62	0.28	0.14	0.03	0.41	0.07	0.65	nd	0.22	0.34	0.54	0.10
Zooplankton	Night	0.2-0.5 mm	25	-16.21	-6.88	-8.04	1.33	-24.10	-29.32	-20.28	-18.09	-14.20	nd	-14.55	-26.27	-25.86	-20.26	0.18	0.18	0.17	0.61	0.08	0.20	0.58	0.29	0.19	nd	0.63	0.42	0.25	1.22
Zooplankton	Night	1-2 mm	25	-17.70	-9.60	-10.90	-3.40	-24.90	-29.50	-19.30	-18.80	-15.30	nd	-15.50	-25.60	-24.40	-20.40	0.50	0.23	0.60	0.22	0.22	0.09	0.69	0.15	0.33	nd	0.11	0.15	0.05	0.33
Zooplankton	Night	2-5 mm	25	-18.76	-11.00	-13.87	-7.48	-29.04	-30.89	-21.43	-20.23	-18.24	-22.38	-19.21	-27.62	-26.36	-20.25	0.95	0.82	0.41	0.48	0.48	0.65	0.28	0.10	0.40	0.64	0.36	0.36	0.74	0.05
Zooplankton	Night	5 mm	25	-19.79	-8.95	-14.71	-6.47	-29.62	-31.36	-22.54	-20.70	-18.73	-22.72	-19.26	-27.79	-26.13	-20.94	0.34	0.61	0.86	0.24	0.24	0.19	0.29	0.13	0.04	0.14	0.21	0.20	0.34	0.13
Metridia	Night	1-2 mm	25	-23.12	-13.43	-18.39	-10.25	-31.60	-33.00	-24.70	-22.47	-20.58	-24.16	-20.81	-28.73	nd	-19.24	0.59	0.38	0.49	0.15	0.42	0.46	0.12	0.05	0.37	0.23	0.34	0.07	nd	0.29
Neocalanus	Night	1-2 mm	625	-17.88	-9.48	-13.93	-5.39	-30.29	-31.76	-22.62	-20.47	-18.98	nd	-19.16	-27.78	nd	-19.45	0.25	0.49	0.33	0.50	0.12	0.07	0.22	0.36	0.35	nd	0.31	0.10	nd	0.45
Chaetognath	Night	2-5 mm	625	-20.74	-5.59	-15.29	-2.80	-30.14	-32.46	-24.22	-21.67	-19.56	-23.48	-19.02	-28.42	nd	-20.45	0.34	0.37	0.17	0.35	0.52	0.14	0.30	0.05	0.28	0.66	0.07	0.13	nd	0.11
Chaetognath	Night	5 mm	625	-22.71	-8.70	-18.13	-9.23	-31.33	-33.06	-25.25	-22.35	-20.80	-23.68	-20.13	-28.85	nd	-21.27	0.56	1.18	0.13	0.93	0.17	0.35	0.35	0.27	0.11	0.61	0.53	0.41	nd	0.86
Chaetognath	Night	2-5 mm	350	-22.33	-8.61	-15.90	-4.54	-30.59	-32.22	-24.32	-21.51	-20.50	-23.72	-18.66	-28.78	nd	-20.35	0.18	0.36	0.46	0.14	0.36	0.18	0.15	0.14	0.17	0.79	0.27	0.08	nd	0.31
Chaetognath	Night	5 mm	350	-20.77	-5.35	-16.38	-0.25	-30.29	-32.39	-24.30	-21.32	-20.07	-23.54	-19.25	-28.96	nd	-20.06	0.39	0.21	0.26	0.67	0.46	0.12	0.35	0.31	0.08	0.67	0.07	0.16	nd	0.16
Radiolarian	Day	5 mm	625	-21.39	-9.45	-14.43	-5.10	-29.26	-31.04	-23.08	-20.62	-20.13	-58.03	-19.61	-28.65	-26.06	-21.73	0.12	0.08	0.54	0.85	0.31	0.24	0.31	0.16	0.02	0.16	0.34	0.22	0.24	0.09
Radiolarian	Night	5 mm	625	-20.65	-8.99	-13.97	-3.48	-28.65	-30.74	-22.70	-19.99	-19.38	nd	-19.62	-27.84	-26.34	-21.88	0.19	0.27	0.60	0.54	0.22	0.15	0.05	0.02	0.27	nd	0.30	0.32	0.64	0.39

Table 9: δ^{15}N values of particles collected by in-situ filtration and sediment traps.

				δ^{15}N (‰)													SD (‰)													
Type	Event	Size	Depth	Ala	Gly	Thr	Ser	Val	Leu	Iso	Pro	Asx	Met	Glx	Phe	Tyr	Lys	Ala	Gly	Thr	Ser	Val	Leu	Ile	Pro	Asx	Met	Glx	Phe	Tyr	Lys
Particle	Epoch 1	1-6 um	500	14.90	2.61	-4.85	2.72	10.76	10.08	11.31	9.78	11.67	nd	15.81	5.24	2.47	1.98	nd	3.51	1.11	1.89	-1.04	0.20	0.88	0.17	0.20	0.42	0.68	1.16	0.50	0.20
Particle	Epoch 1	1-6 um	195	15.26	3.12	-4.31	2.76	12.58	10.36	11.96	11.33	12.04	nd	16.41	6.09	5.08	3.45	nd	13.94	4.06	-5.15	2.33	2.17	0.49	0.90	1.00	1.00	0.54	1.00	0.17	1.76
Particle	Epoch 1	1-6 um	145	9.65	0.79	-5.27	0.24	8.47	6.07	6.17	7.99	8.40	nd	12.16	3.89	3.41	3.05	2.44	11.07	3.16	4.41	2.82	0.20	0.16	0.22	0.50	0.20	0.20	0.33	0.16	0.20
Particle	Epoch 1	Trap	145	14.01	0.26	-11.86	0.79	8.89	8.45	9.16	9.04	8.69	nd	14.17	1.44	2.53	-0.84	nd	nd	nd	nd	nd	nd	nd	nd	nd	nd	nd	nd	nd	nd
Particle	Epoch 1	1-6 um	95	5.55	-1.61	-5.24	-3.71	4.92	1.73	3.13	2.84	5.15	nd	6.88	1.37	1.87	0.33	0.69	7.89	0.85	1.67	0.95	0.43	0.20	0.29	0.20	0.41	0.20	0.20	0.26	0.22
Particle	Epoch 1	1-6 um	50	2.73	-3.20	-7.11	-5.49	2.48	-0.63	-0.38	0.42	1.64	nd	3.53	-0.82	0.65	-1.54	nd	8.00	1.10	-0.40	0.75	0.21	0.20	0.60	0.20	0.33	0.38	0.20	0.33	0.42
Particle	Epoch 2	1-6 um	500	18.13	2.99	-5.76	2.98	13.35	11.88	13.28	11.98	13.83	nd	17.66	4.84	6.76	5.24	nd	15.81	5.24	2.47	1.98	0.53	0.27	0.28	0.20	0.98	0.20	0.68	0.45	0.34
Particle	Epoch 2	1-6 um	330	17.54	2.47	-6.17	2.15	13.25	11.19	12.13	10.91	12.48	nd	17.12	5.37	6.43	5.04	nd	18.44	4.92	nd	3.00	0.24	0.29	1.69	0.81	0.69	0.36	0.81	0.72	0.73
Particle	Epoch 2	51 um	320	13.97	1.25	-8.02	-0.19	9.92	9.12	8.50	8.16	9.03	nd	11.85	1.83	-1.56	-1.35	nd	4.62	-0.36	2.26	-2.23	0.20	0.20	0.69	0.23	0.23	0.20	0.20	0.50	0.20
Particle	Epoch 2	1-6 um	320	14.56	2.92	-7.13	2.34	11.97	10.78	11.63	11.14	10.96	nd	15.79	4.34	8.01	3.70	nd	15.73	6.78	6.25	4.87	0.60	0.20	0.61	0.44	0.29	0.49	0.48	0.33	0.20
Particle	Epoch 2	6-51 um	320	12.78	0.91	-6.85	-0.17	8.86	8.34	7.31	7.70	8.54	nd	12.24	2.58	-0.56	-0.22	nd	10.16	3.64	nd	0.07	1.00	1.00	1.00	1.00	1.00	1.00	1.00	1.00	1.00
Particle	Epoch 2	6-51 um	320	10.22	-0.05	0.54	-1.71	7.56	4.18	1.99	4.70	7.30	nd	10.16	3.64	nd	0.07	nd	8.59	0.84	4.18	2.06	1.00	1.00	1.00	1.00	1.00	1.00	1.00	1.00	1.00
Particle	Epoch 2	1-6 um	195	12.84	1.82	-5.50	2.46	9.72	9.40	10.12	11.18	11.43	5.12	15.00	5.19	7.45	5.00	nd	16.41	6.09	5.08	3.45	1.15	0.53	1.55	0.99	0.91	0.61	0.52	0.57	1.12
Particle	Epoch 2	1-6 um	145	13.79	0.96	-5.60	0.86	10.79	6.76	7.60	8.97	9.97	nd	12.89	3.31	4.31	3.15	nd	12.16	3.89	3.41	3.05	0.90	0.65	0.90	0.92	0.68	0.46	1.01	1.01	0.75
Particle	Epoch 2	1-6 um	95	9.14	4.19	-3.12	-3.01	5.74	3.88	3.14	3.50	6.42	nd	8.00	1.10	-0.40	0.75	nd	6.88	1.37	1.87	0.33	0.88	0.72	0.75	0.52	1.52	0.20	0.58	0.37	0.77
Particle	Epoch 2	51 um	85	15.20	1.52	-9.59	2.36	11.40	11.04	9.33	10.39	11.70	nd	15.36	1.90	4.92	0.78	nd	15.02	2.78	0.54	1.82	1.14	1.37	0.50	1.80	2.04	0.92	0.49	1.32	0.93
Particle	Epoch 2	0.3-1.0 um	85	10.12	-1.66	2.80	-3.74	7.35	3.96	3.71	5.30	8.19	nd	8.86	2.10	4.96	4.01	nd	5.40	1.22	2.53	1.22	0.21	0.71	0.68	0.29	1.09	0.67	0.20	0.45	0.20
Particle	Epoch 2	1-6 um	85	13.35	1.05	-0.91	0.37	9.35	5.09	5.95	7.30	9.04	nd	9.42	2.20	4.24	3.17	nd	15.79	4.34	8.01	3.70	0.38	0.46	0.58	0.75	0.75	0.25	0.88	0.55	0.53
Particle	Epoch 2	6-51 um	85	12.21	1.33	-4.63	0.24	8.33	7.83	6.55	6.90	9.97	nd	12.55	2.86	5.11	1.38	nd	12.24	2.58	-0.56	-0.22	0.53	0.18	0.39	1.16	0.60	0.39	0.34	0.35	0.29
Particle	Epoch 2	1-6 um	50	4.27	-1.43	-4.01	-5.18	2.16	1.25	-0.40	1.67	3.26	-0.57	4.77	-1.18	-1.86	-0.57	nd	3.53	-0.82	0.65	-1.54	0.53	0.60	1.09	0.80	0.67	0.29	1.23	0.61	0.72
Particle	Epoch 2	51 um	20	5.19	3.13	0.34	-1.61	7.03	3.74	2.59	1.98	6.47	nd	7.51	1.21	2.60	1.53	nd	15.36	1.90	4.92	0.78	1.00	1.00	1.00	1.00	1.00	1.00	1.00	1.00	1.00
Particle	Epoch 2	0.3-1.0 um	20	2.57	-2.68	-4.64	-5.52	1.82	-0.09	-0.71	0.86	0.93	nd	4.62	-0.36	2.26	-2.23	nd	2.67	-0.21	0.13	-0.59	0.20	0.20	0.71	0.20	0.19	0.20	0.20	0.20	0.27
Particle	Epoch 2	1-6 um	20	4.16	-1.61	-4.46	-4.18	3.59	1.16	0.08	2.11	2.87	nd	3.51	1.11	1.89	-1.04	0.38	3.39	0.73	2.62	0.02	0.65	0.46	0.21	0.33	0.39	0.37	0.66	0.39	0.21
Particle	Epoch 2	6-51 um	20	5.35	-0.46	-4.20	-2.85	4.88	3.44	1.49	2.44	3.64	nd	6.96	0.18	2.63	-2.10	nd	12.55	2.86	5.11	1.38	0.20	0.20	0.20	0.30	0.87	0.42	0.75	0.26	0.81
Particle	Epoch 3	51 um	320	12.18	0.48	-7.51	0.56	11.74	8.71	9.18	8.25	8.78	nd	15.02	2.78	0.54	1.82	nd	11.85	1.83	-1.56	-1.35	0.18	0.52	0.36	0.80	0.52	0.46	0.65	0.19	0.32
Particle	Epoch 3	0.3-1.0 um	320	18.97	9.29	9.28	8.93	17.62	11.97	13.99	14.11	15.08	nd	17.16	12.18	nd	10.09	nd	14.70	10.06	10.47	6.79	0.43	0.26	0.39	0.69	0.35	0.20	0.45	0.30	0.45
Particle	Epoch 3	0.3-1.0 um	320	17.80	4.99	8.31	6.50	15.81	10.13	11.32	12.67	12.51	nd	14.70	10.06	10.47	6.79	nd	14.17	1.44	2.53	-0.84	0.34	0.50	0.78	0.62	0.50	0.19	0.25	0.37	0.20
Particle	Epoch 3	1-6 um	320	17.38	4.02	-3.44	2.55	12.32	12.23	12.27	10.77	13.26	nd	15.73	6.78	6.25	4.87	nd	6.34	-0.13	nd	0.33	1.00	1.00	1.00	1.00	1.00	1.00	1.00	1.00	1.00
Particle	Epoch 3	6-51 um	320	11.63	2.21	-5.92	1.47	8.48	7.26	8.19	9.19	8.81	nd	11.17	1.62	5.26	2.25	nd	13.56	2.48	nd	0.75	0.90	0.35	0.51	0.15	1.90	0.64	0.23	0.76	0.44
Particle	Epoch 3	1-6 um	205	12.52	0.38	-4.56	3.26	13.47	9.01	10.06	9.21	10.58	nd	13.94	4.06	-5.15	2.33	nd	17.12	5.37	6.43	5.04	0.38	0.28	0.59	0.38	0.29	0.20	0.32	0.29	0.32
Particle	Epoch 3	1-6 um	155	9.52	0.46	-5.45	0.79	8.01	5.85	7.32	7.55	8.69	2.44	11.07	3.16	4.41	2.82	5.12	15.00	5.19	7.45	5.00	1.00	1.00	1.00	1.00	1.00	1.00	1.00	1.00	1.00
Particle	Epoch 3	1-6 um	105	5.37	-2.03	-4.62	-2.91	5.24	2.33	3.71	3.71	5.69	0.69	7.89	0.85	1.67	0.95	nd	12.89	3.31	4.31	3.15	1.33	0.79	0.83	0.60	0.51	0.79	0.40	0.40	0.49
Particle	Epoch 3	1-6 um	50	4.72	-1.94	-2.05	-2.36	5.72	2.23	2.65	4.60	4.59	nd	5.40	1.22	2.53	1.22	-0.57	4.77	-1.18	-1.86	-0.57	0.18	0.22	0.39	0.20	0.16	0.29	0.44	0.20	0.20
Particle	Epoch 3	51 um	20	6.49	1.31	1.02	-0.44	7.18	2.95	2.32	2.55	4.44	nd	6.55	2.18	2.29	2.11	nd	7.51	1.21	2.60	1.53	0.20	0.32	0.28	0.20	0.20	0.48	0.50	0.20	1.24
Particle	Epoch 3	0.3-1.0 um	20	3.21	-2.77	-4.08	-4.43	1.46	0.64	0.26	2.07	1.82	nd	2.67	-0.21	0.13	-0.59	nd	8.86	2.10	4.96	4.01	0.20	0.21	0.20	0.20	0.20	0.23	0.92	0.47	0.26
Particle	Epoch 3	1-6 um	20	3.19	-1.45	-3.44	-4.06	2.89	0.93	1.36	2.58	2.90	0.38	3.39	0.73	2.62	0.02	nd	9.42	2.20	4.24	3.17	0.44	0.71	0.22	0.54	0.29	0.54	0.23	0.20	0.21
Particle	Epoch 3	6-51 um	20	9.60	2.63	0.76	-0.86	5.37	3.14	1.66	2.34	4.71	nd	8.59	0.84	4.18	2.06	nd	11.17	1.62	5.26	2.25	1.00	1.00	1.00	1.00	1.00	1.00	1.00	1.00	1.00
Trap	Epoch 1	Trap	500	13.45	3.48	-10.97	2.68	8.37	9.12	7.86	10.22	9.94	nd	14.28	1.60	5.04	0.94	nd	17.16	12.18	nd	10.09	0.49	1.30	0.85	0.97	0.29	0.24	0.22	0.78	0.90
Trap	Epoch 1	Trap	330	12.69	-1.15	-13.65	1.28	10.36	7.92	8.33	7.11	8.14	nd	9.36	0.99	-2.10	-0.25	nd	14.28	1.60	5.04	0.94	0.49	0.47	0.18	1.52	1.13	0.35	0.22	0.78	0.98
Trap	Epoch 1	Trap	195	17.14	-0.11	-12.72	-0.30	9.59	8.20	8.15	8.26	9.16	nd	13.93	3.66	0.88	-0.01	nd	9.36	0.99	-2.10	-0.25	0.97	1.36	0.28	0.74	0.20	0.20	0.20	0.29	0.43
Trap	Epoch 1	Trap	95	13.14	0.07	-10.61	1.03	10.83	8.14	9.08	7.18	8.30	nd	13.56	2.48	nd	0.75	nd	12.47	1.60	nd	0.60	0.51	0.51	0.39	0.54	0.29	0.20	0.68	0.56	0.53
Trap	Epoch 3	Trap	104	13.83	1.26	-11.44	0.62	8.66	10.06	10.12	9.67	8.86	nd	12.47	1.60	nd	0.60	nd	13.93	3.66	0.88	-0.01	0.81	1.53	0.43	0.54	0.98	0.20	1.30	0.42	0.85

References

Archibald, K. M., D. A. Siegel, and S. C. Doney (2019). Modeling the impact of zooplankton diel vertical migration on the carbon export flux of the biological pump. *Global Biogeochemical Cycles 33*(2), 181–199.

Arthur, K. E., S. Kelez, T. Larsen, C. A. Choy, and B. N. Popp (2014). Tracing the biosynthetic source of essential amino acids in marine turtles using δ13c fingerprints. *Ecology 95*(5), 1285–1293.

Behrenfeld, M. J., E. Boss, D. A. Siegel, and D. M. Shea (2005). Carbon-based ocean productivity and phytoplankton physiology from space. *Global biogeochemical cycles 19*(1).

Bode, A., M. P. Olivar, and S. Hernández-León (2021). Trophic indices for micronektonic fishes reveal their dependence on the microbial system in the north atlantic. *Scientific reports 11*(1), 1–10.

Boyd, P., N. Sherry, J. Berges, J. Bishop, S. Calvert, M. Charette, S. Giovannoni, R. Goldblatt, P. Harrison, S. Moran, et al. (1999). Transformations of biogenic particulates from the pelagic to the deep ocean realm. *Deep Sea Research Part II: Topical Studies in Oceanography 46*(11-12), 2761–2792.

Bradley, C. J., N. J. Wallsgrove, C. A. Choy, J. C. Drazen, E. D. Hetherington, D. K. Hoen, and B. N. Popp (2015). Trophic position estimates of marine teleosts using amino acid compound specific isotopic analysis. *Limnology and oceanography: Methods 13*(9), 476–493.

Buesseler, K. O., C. R. Benitez-Nelson, M. Roca-Martí, A. M. Wyatt, L. Resplandy, S. J. Clevenger, J. A. Drysdale, M. L. Estapa, S. Pike, and B. P. Umhau (2020). High-resolution spatial and temporal measurements of particulate organic carbon flux using thorium-234 in the northeast pacific ocean during the export processes in the ocean from remote sensing field campaign. *Elementa: Science of the Anthropocene 8*(1).

Buesseler, K. O., P. W. Boyd, E. E. Black, and D. A. Siegel (2020). Metrics that matter for assessing the ocean biological carbon pump. *Proceedings of the National Academy of Sciences 117*(18), 9679–9687.

Burd, A. B., D. A. Hansell, D. K. Steinberg, T. R. Anderson, J. Arístegui, F. Baltar, S. R. Beaupre, K. O. Buesseler, F. DeHairs, G. A. Jackson, et al. (2010). Assessing the apparent imbalance between geochemical and biochemical indicators of meso-and bathypelagic biological activity: What the $* * **$ is wrong with present calculations of carbon budgets? *Deep Sea Research Part II: Topical Studies in Oceanography 57*(16), 1557–1571.

Calbet, A. and M. R. Landry (2004). Phytoplankton growth, microzooplankton grazing, and carbon cycling in marine systems. *Limnology and Oceanography 49*(1), 51–57.

Chikaraishi, Y., N. O. Ogawa, Y. Kashiyama, Y. Takano, H. Suga, A. Tomitani, H. Miyashita, H. Kitazato, and N. Ohkouchi (2009). Determination of aquatic food-web structure based on compound-specific nitrogen isotopic composition of amino acids. *Limnology and Oceanography: methods 7*(11), 740–750.

Décima, M. and M. R. Landry (2020). Resilience of plankton trophic structure to an eddy-stimulated diatom bloom in the north pacific subtropical gyre. *Marine Ecology Progress Series 643*, 33–48.

Décima, M., M. R. Landry, C. J. Bradley, and M. L. Fogel (2017). Alanine δ15n trophic fractionation in heterotrophic protists. *Limnology and Oceanography 62*(5), 2308–2322.

Doherty, S. C., A. E. Maas, D. K. Steinberg, B. N. Popp, and H. G. Close (2021). Distinguishing zooplankton fecal pellets as a component of the biological pump using compound-specific isotope analysis of amino acids. *Limnology and Oceanography*.

Ducklow, H. W., D. K. Steinberg, and K. O. Buesseler (2001). Upper ocean carbon export and the biological pump. *OCEANOGRAPHY-WASHINGTON DC-OCEANOGRAPHY SOCIETY- 14*(4), 50–58.

Estapa, M. L., C. A. Durkin, M. Omand, and K. Buesseler (2020). Diagnosing export pathways in the biological pump: Sediment trap data from the exports north pacific field campaign. In *Ocean Sciences Meeting 2020*. Agu.

Gloeckler, K., C. A. Choy, C. C. Hannides, H. G. Close, E. Goetze, B. N. Popp, and J. C. Drazen (2018). Stable isotope analysis of micronekton around hawaii reveals suspended particles are an

important nutritional source in the lower mesopelagic and upper bathypelagic zones. *Limnology and Oceanography 63*(3), 1168–1180.

Goldblatt, R. H., D. L. Mackas, and A. G. Lewis (1999). Mesozooplankton community characteristics in the ne subarctic pacific. *Deep Sea Research Part II: Topical Studies in Oceanography 46*(11-12), 2619–2644.

Gutiérrez-Rodríguez, A., M. Décima, B. N. Popp, and M. R. Landry (2014). Isotopic invisibility of protozoan trophic steps in marine food webs. *Limnology and oceanography 59*(5), 1590–1598.

Hannides, C. C., B. N. Popp, C. A. Choy, and J. C. Drazen (2013). Midwater zooplankton and suspended particle dynamics in the north pacific subtropical gyre: A stable isotope perspective. *Limnology and Oceanography 58*(6), 1931–1946.

Hannides, C. C., B. N. Popp, H. G. Close, C. R. Benitez-Nelson, A. Cassie, K. Gloeckler, N. Wallsgrove, B. Umhau, E. Palmer, and J. C. Drazen (2020). Seasonal dynamics of midwater zooplankton and relation to particle cycling in the north pacific subtropical gyre. *Progress in Oceanography 182*, 102266.

Hannides, C. C., B. N. Popp, M. R. Landry, and B. S. Graham (2009). Quantification of zooplankton trophic position in the north pacific subtropical gyre using stable nitrogen isotopes. *Limnology and oceanography 54*(1), 50–61.

Harrison, P., P. Boyda, D. Varela, S. Takeda, A. Shiomoto, and T. Odate (1999). Comparison of factors controlling phytoplankton productivity in the ne and nw subarctic pacific gyres. *Progress in Oceanography 43*(2-4), 205–234.

Herndl, G. J. and T. Reinthaler (2013). Microbial control of the dark end of the biological pump. *Nature geoscience 6*(9), 718.

Jarman, C. L., T. Larsen, T. Hunt, C. Lipo, R. Solsvik, N. Wallsgrove, C. Ka'apu-Lyons, H. G. Close, and B. N. Popp (2017). Diet of the prehistoric population of rapa nui (easter island, chile) shows environmental adaptation and resilience. *American journal of physical anthropology 164*(2), 343–361.

Kruse, S., T. Brey, and U. Bathmann (2010). Role of midwater chaetognaths in southern ocean pelagic energy flow. *Marine Ecology Progress Series 416*, 105–113.

Lam, P. J., D. C. Ohnemus, and M. E. Auro (2015). Size-fractionated major particle composition and concentrations from the us geotraces north atlantic zonal transect. *Deep Sea Research Part II: Topical Studies in Oceanography 116*, 303–320.

Landry, M. R. and M. R. Décima (2017). Protistan microzooplankton and the trophic position of tuna: quantifying the trophic link between micro-and mesozooplankton in marine foodwebs. *ICES Journal of Marine Science 74*(7), 1885–1892.

Landry, M. R., B. C. Monger, and K. E. Selph (1993). Time-dependency of microzooplankton grazing and phytoplankton growth in the subarctic pacific. *Progress in Oceanography 32*(1-4), 205–222.

Landry, M. R., K. E. Selph, M. R. Stukel, R. Swalethorp, T. B. Kelly, J. L. Beatty, and C. R. Quackenbush (2021). Microbial food web dynamics in the oceanic gulf of mexico. *Journal of Plankton Research*.

Larsen, T., D. L. Taylor, M. B. Leigh, and D. M. O'Brien (2009). Stable isotope fingerprinting: a novel method for identifying plant, fungal, or bacterial origins of amino acids. *Ecology 90*(12), 3526–3535.

Larsen, T., M. Ventura, N. Andersen, D. M. O'Brien, U. Piatkowski, and M. D. McCarthy (2013). Tracing carbon sources through aquatic and terrestrial food webs using amino acid stable isotope fingerprinting. *PloS one 8*(9), e73441.

Mackas, D. L., R. Goldblatt, and A. G. Lewis (1998). Interdecadal variation in developmental timing of neocalanus plumchrus populations at ocean station p in the subarctic north pacific. *Canadian Journal of Fisheries and Aquatic Sciences 55*(8), 1878–1893.

Mayor, D. J., R. Sanders, S. L. Giering, and T. R. Anderson (2014). Microbial gardening in the ocean's twilight zone: Detritivorous metazoans benefit from fragmenting, rather than ingesting, sinking detritus: Fragmentation of refractory detritus by zooplankton beneath the

euphotic zone stimulates the harvestable production of labile and nutritious microbial biomass. *Bioessays 36*(12), 1132–1137.

McCarthy, M. D., R. Benner, C. Lee, and M. L. Fogel (2007). Amino acid nitrogen isotopic fractionation patterns as indicators of heterotrophy in plankton, particulate, and dissolved organic matter. *Geochimica et Cosmochimica Acta 71*(19), 4727–4744.

McClelland, J. W. and J. P. Montoya (2002). Trophic relationships and the nitrogen isotopic composition of amino acids in plankton. *Ecology 83*(8), 2173–2180.

McMahon, K. W., S. R. Thorrold, L. A. Houghton, and M. L. Berumen (2016). Tracing carbon flow through coral reef food webs using a compound-specific stable isotope approach. *Oecologia 180*(3), 809–821.

McNair, H. M. and S. Menden-Deuer (2020). Protist grazing contributes to microbial food web at the upper boundary of the twilight zone in the subarctic pacific. *Marine Ecology Progress Series 636*, 235–241.

McNair, H. M., F. Morison, J. R. Graff, T. A. Rynearson, and S. Menden-Deuer (2021). Microzooplankton grazing constrains pathways of carbon export in the subarctic north pacific. *Limnology and Oceanography*.

Mével, G., M. Vernet, M. Goutx, and J. F. Ghiglione (2008). Seasonal to hour variation scales in abundance and production of total and particle-attached bacteria in the open nw mediterranean sea (0–1000 m). *Biogeosciences 5*(6), 1573–1586.

Miller, C. B. (1993). Pelagic production production in the subacrtic pacific. *Progress in Oceanography 32*(1-4), 1–15.

Miller, C. B., B. W. Frost, P. A. Wheeler, M. R. Landry, N. Welschmeyer, and T. M. Powell (1991). Ecological dynamics in the subarctic pacific, a possibly iron-limited ecosystem. *Limnology and Oceanography 36*(8), 1600–1615.

Ohkouchi, N., Y. Chikaraishi, H. G. Close, B. Fry, T. Larsen, D. J. Madigan, M. D. McCarthy, K. W. McMahon, T. Nagata, Y. I. Naito, et al. (2017). Advances in the application of amino acid

nitrogen isotopic analysis in ecological and biogeochemical studies. *Organic Geochemistry 113*, 150–174.

Owens, S., S. Pike, and K. Buesseler (2015). Thorium-234 as a tracer of particle dynamics and upper ocean export in the atlantic ocean. *Deep Sea Research Part II: Topical Studies in Oceanography 116*, 42–59.

Phillips, D. L. and J. W. Gregg (2001). Uncertainty in source partitioning using stable isotopes. *Oecologia 127*(2), 171–179.

Popp, B. N., B. S. Graham, R. J. Olson, C. C. Hannides, M. J. Lott, G. A. López-Ibarra, F. Galván-Magaña, and B. Fry (2007). Insight into the trophic ecology of yellowfin tuna, thunnus albacares, from compound-specific nitrogen isotope analysis of proteinaceous amino acids. *Terrestrial Ecology 1*, 173–190.

R Core Team (2018). *R: A Language and Environment for Statistical Computing*. Vienna, Austria: R Foundation for Statistical Computing.

Reinthaler, T., H. Van Aken, C. Veth, J. Arístegui, C. Robinson, P. J. l. B. Williams, P. Lebaron, and G. J. Herndl (2006). Prokaryotic respiration and production in the meso-and bathypelagic realm of the eastern and western north atlantic basin. *Limnology and Oceanography 51*(3), 1262–1273.

Ripley, B., B. Venables, D. M. Bates, K. Hornik, A. Gebhardt, D. Firth, and M. B. Ripley (2013). Package 'mass'. *Cran r 538*, 113–120.

Robinson, C., D. K. Steinberg, T. R. Anderson, J. Aristegui, C. A. Carlson, J. R. Frost, J.-F. Ghiglione, S. Hernandez-Leon, G. A. Jackson, R. Koppelmann, et al. (2010). Mesopelagic zone ecology and biogeochemistry–a synthesis. *Deep Sea Research Part II: Topical Studies in Oceanography 57*(16), 1504–1518.

Romero-Romero, S., C. A. Ka'apu-Lyons, B. P. Umhau, C. R. Benitez-Nelson, C. C. Hannides, H. G. Close, J. C. Drazen, and B. N. Popp (2020). Deep zooplankton rely on small particles when particle fluxes are low. *Limnology and Oceanography Letters*.

Saito, H. and T. Kiørboe (2001). Feeding rates in the chaetognath sagitta elegans: effects of prey size, prey swimming behaviour and small-scale turbulence. *Journal of Plankton Research 23*(12), 1385–1398.

Scott, J. H., D. M. O'Brien, D. Emerson, H. Sun, G. D. McDonald, A. Salgado, and M. L. Fogel (2006). An examination of the carbon isotope effects associated with amino acid biosynthesis. *Astrobiology 6*(6), 867–880.

Siegel, D. A., K. Buesseler, M. Behrenfeld, C. Benitez-Nelson, E. Boss, M. Brzezinski, A. Burd, C. Carlson, E. D'Asaro, S. Doney, M. Perry, R. Stanley, and D. Steinberg (2015). Export processes in the ocean from remote sensing (exports): A science plan for a nasa field campaign.

Siegel, D. A., K. Buesseler, S. C. Doney, S. Sailley, M. J. Behrenfeld, and P. Boyd (2014). Global assessment of ocean carbon export by combining satellite observations and food-web models. *Global Biogeochemical Cycles 28*(3), 181–196.

Siegel, D. A., I. Cetinić, J. R. Graff, C. M. Lee, N. Nelson, M. J. Perry, I. S. Ramos, D. K. Steinberg, K. Buesseler, R. Hamme, et al. (2021). An operational overview of the export processes in the ocean from remote sensing (exports) northeast pacific field deployment. *Elementa: Science of the Anthropocene 9*(1).

Silfer, J., M. Engel, S. Macko, and E. Jumeau (1991). Stable carbon isotope analysis of amino acid enantiomers by conventional isotope ratio mass spectrometry and combined gas chromatography/isotope ratio mass spectrometry. *Analytical Chemistry 63*(4), 370–374.

Steinberg, D. K., C. A. Carlson, N. R. Bates, S. A. Goldthwait, L. P. Madin, and A. F. Michaels (2000). Zooplankton vertical migration and the active transport of dissolved organic and inorganic carbon in the sargasso sea. *Deep Sea Research Part I: Oceanographic Research Papers 47*(1), 137–158.

Steinberg, D. K., J. S. Cope, S. E. Wilson, and T. Kobari (2008). A comparison of mesopelagic mesozooplankton community structure in the subtropical and subarctic north pacific ocean. *Deep Sea Research Part II: Topical Studies in Oceanography 55*(14-15), 1615–1635.

Steinberg, D. K. and M. R. Landry (2017). Zooplankton and the ocean carbon cycle. *Annual Review of Marine Science 9*, 413–444.

Steinberg, D. K., B. A. Van Mooy, K. O. Buesseler, P. W. Boyd, T. Kobari, and D. M. Karl (2008). Bacterial vs. zooplankton control of sinking particle flux in the ocean's twilight zone. *Limnology and Oceanography 53*(4), 1327–1338.

Strzepek, R. F. and P. J. Harrison (2004). Photosynthetic architecture differs in coastal and oceanic diatoms. *Nature 431*(7009), 689–692.

Taylor, J. (1997). *Introduction to error analysis, the study of uncertainties in physical measurements*.

Terazaki, M. (1995). The role of carnivorous zooplankton, particularly chaetognaths in ocean flux. *Biogeochemical Processes and Ocean Flux in the Western Pacific*, 319–330.

Umhau, B. P., C. R. Benitez-Nelson, H. G. Close, C. C. Hannides, L. Motta, B. N. Popp, J. D. Blum, and J. C. Drazen (2019). Seasonal and spatial changes in carbon and nitrogen fluxes estimated using 234th: 238u disequilibria in the north pacific tropical and subtropical gyre. *Marine Chemistry 217*, 103705.

Wall, C. B., N. J. Wallsgrove, R. D. Gates, and B. N. Popp (2021). Amino acid δ13c and δ15n analyses reveal distinct species-specific patterns of trophic plasticity in a marine symbiosis. *Limnology and Oceanography 66*(5), 2033–2050.

Wiebe, P., A. Morton, A. Bradley, R. Backus, J. Craddock, V. Barber, T. Cowles, and G. d. . Flierl (1985). New development in the mocness, an apparatus for sampling zooplankton and micronekton. *Marine Biology 87*(3), 313–323.

Yamaguchi, Y. T., Y. Chikaraishi, Y. Takano, N. O. Ogawa, H. Imachi, Y. Yokoyama, and N. Ohkouchi (2017). Fractionation of nitrogen isotopes during amino acid metabolism in heterotrophic and chemolithoautotrophic microbes across eukarya, bacteria, and archaea: effects of nitrogen sources and metabolic pathways. *Organic Geochemistry 111*, 101–112.

Yamaguchi, Y. T. and M. D. McCarthy (2018). Sources and transformation of dissolved and particulate organic nitrogen in the north pacific subtropical gyre indicated by compound-specific δ15n analysis of amino acids. *Geochimica et Cosmochimica Acta 220*, 329–347.